Space Science Reviews (2026) 222:78
https://doi.org/10.1007/s11214-026-01334-2

Transients and Stellar Activity as Revealed by Ultraviolet Diagnostic Tracers

Richard de Grijs[1,2,3] · Martin A. Barstow[4] · Deepak Chahal[1,2,5] · Fabio Favata[6,7,3] · Xiaoting Fu[8] · Ana I. Gómez de Castro[9] · Sipra Hota[10,11] · Firoza Sutaria[10]

Received: 28 November 2025 / Accepted: 13 October 2026
© The Author(s) 2026

Abstract
Ultraviolet (UV) observations offer unique insights into transient and variable astrophysical phenomena, from the Sun and nearby stars to supernovae and star-forming galaxies. Here, we summarise and review the diagnostic power of the UV spectrum for probing the physical conditions, dynamics and energetics of these events. We trace the historical development of UV astronomy from early satellite missions to the current landscape shaped by the Hubble Space Telescope, the GALaxy Evolution eXplorer, the Neil Gehrels Swift Observatory and *AstroSat*/UVIT. Particular emphasis is placed on resonance lines such as Mg II *h* and *k*, C II, Si IV, C IV and N V, which probe the (solar and) stellar chromosphere and transition region, revealing magnetic heating, shocks and mass loss across stellar types. We examine UV diagnostics of stellar flares, pre-main-sequence activity and rotation–activity correlations, linking them to exoplanetary irradiation and habitability. We then explore the UV view of supernova shock breakout and early-time emission, as well as the far-UV mapping of young stellar populations and hierarchical star formation in the Magellanic Clouds. Together, these aspects illustrate how the UV connects small-scale plasma processes to galactic-scale star formation. Despite remarkable progress, UV transient astronomy remains limited by instrument availability and cadence. Forthcoming missions promise to transform this field by capturing the rapid, luminous phenomena that define the dynamic Universe.

1 Setting the Scene

From its inception, the exploration of the Universe at ultraviolet (UV) wavelengths has been driven by a dual desire: (i) to access the rich forest of atomic and ionic transitions that fall in this spectral range and (ii) to exploit these diagnostics to reveal the dynamic processes shaping stars and the galaxies they form. Here, we will adopt the conventional astronomical definitions of the UV regime. The UV broadly encompasses wavelengths from ∼100 to 4000 Å, bridging the optical domain and the soft X-ray regime. For clarity, we refer to the near-UV as the interval from approximately 2000 to 4000 Å, where chromospheric and upper-photospheric diagnostics dominate. The far-UV, spanning ∼912–2000 Å, contains key resonance lines (e.g., C IV, Si IV, N V) that trace transition-region plasma and radiatively driven winds. At still shorter wavelengths, the extreme-UV (∼100–912 Å) probes highly ionised species in hot (10^{5-6} K) stellar atmospheres, although interstellar H I absorption severely limits extragalactic access to this regime.

Extended author information available on the last page of the article

These spectral subdivisions reflect both physical transitions in stellar atmospheres (e.g., 912 Å corresponds to the hydrogen Lyman limit) and the instrumental capabilities of space-borne UV observatories. In the context of these definitions, for the Sun the upper photosphere corresponds to our star's visible surface, where temperatures are slightly cooler than in the deeper photosphere, roughly 4500–6000 K. The gas density is lower than in deeper photospheric layers, so the plasma is more transparent. The upper photosphere encompasses the first ∼500 km above the solar surface. The chromosphere is located just above the photosphere. It is less dense than the photosphere, with temperatures rising from ∼6000 K at the bottom (some 500 km above the solar surface) to ∼20,000 K at the top, at an altitude of around 2000 km. On top of the chromosphere, the 'transition region' to the tenuous but extremely hot (1–5 MK) corona is very thin, just a few hundred km, but the temperature jumps steeply from ∼20,000 K to ∼500,000 K (see also Sect. 2).

Because the Earth's atmosphere blocks nearly all UV photons, the field's origin coincided with the early Space Age. It has since developed into a cornerstone of stellar astrophysics research, with UV spectroscopy now providing some of the best-constrained tracers of stellar atmospheres, activity and evolution. Here we explore how the UV regime plays a pivotal role in connecting the microphysics of stellar surfaces and coronae to the macroscopic phenomena of stellar variability, explosive transients and even the star-formation histories of galaxies.

The earliest inroads into harnessing UV astronomy were necessarily modest. Suborbital rocket experiments in the 1950s and 1960s, led by pioneering groups in the USA and Europe, delivered the first glimpses of hot-star continua and interstellar absorption features shortwards of 300 nm (Morton and Spitzer 1966). These early spectra demonstrated both the exciting opportunities and the serious challenges associated with UV observations, including, on the one hand, the availability of a wealth of resonance transitions from abundant ions such as C II, Si IV and Mg II; on the other, the technical difficulty of developing stable detectors and reliable calibration above the Earth's atmosphere. Still, these pathfinders laid the foundation for the more ambitious satellite missions that followed, such as the Orbiting Astronomical Observatories (*OAO*) in the late 1960s and early 1970s (Code et al. 1970). *OAO*-2, in particular, showed how UV photometry and low-resolution spectroscopy could be deployed systematically, revealing variations in stellar fluxes and the importance of hot stars in shaping galactic radiation fields (e.g., Code et al. 1970; Code and Meade 1979).

A decisive advance came with *Copernicus* (*OAO*-3), launched in August 1972, which delivered high-resolution stellar UV spectroscopy of unprecedented quality (Rogerson et al. 1973). It opened the door to quantitative studies of interstellar absorption, stellar winds and stellar chromospheric activity. Next, launched in January 1978, the International Ultraviolet Explorer (*IUE*) revolutionised the field by offering a dedicated, long-lived platform for UV spectroscopy. During its operational lifetime (until September 1996), *IUE* collected an enormous archive of UV spectra of both stars and galaxies, its modest aperture compensated by continuous accessibility. For the study of stellar activity (see Sect. 2), *IUE* became a workhorse: the satellite traced variability in chromospheric emission lines, captured flare events and extended solar-inspired diagnostics to large stellar samples (Boggess et al. 1978; Basri et al. 1985).

1.1 The Solar Connection

Although much of the initial UV exploration was motivated by the astrophysics of hot stars and distant galaxies, the Sun quickly emerged as a natural proving ground. The Sun's proximity made it the only object whose UV radiation could be spatially resolved, at least ini-

tially, thus allowing direct tests of theoretical ideas about chromospheric and coronal heating. In the 1960s, early rocket-borne measurements revealed the richness of the solar UV spectrum, with resonance lines such as C II, Si IV, and Mg II *h* and *k* standing out as key diagnostics of temperature, density and velocity fields in the chromosphere and the transition region (Vernazza et al. 1981). These features soon became key diagnostics for interpreting stellar atmospheres more generally, thus ensuring that solar physics and stellar astrophysics research evolved in tandem.

Subsequent satellite observatories deepened this connection. The Orbiting Solar Observatories (*OSO* series) and *Skylab*'s Apollo Telescope Mount provided the first continuous coverage of solar UV emission, documenting its variability across active regions and during flares (Neupert 1965, 1966; Tousey et al. 1977). Later missions such as the Solar and Heliospheric Observatory (*SOHO*) and the Transition Region and Coronal Explorer (*TRACE*) in the 1990s, and the Solar Dynamics Observatory (*SDO*) in the second decade of the current century, refined the picture still further. Their observations demonstrated that solar UV variability is not only a tracer of local magnetic activity but also an important driver of space weather (the influence of solar activity on the near-Earth environment and technological systems), with implications for Earth's ionosphere (an upper atmospheric layer that is ionised by solar and cosmic radiation) and planetary atmospheres more generally (Woods et al. 2000; Pesnell et al. 2012). These insights underlined the dual role of solar UV studies: (i) as a key branch of heliophysics in their own right and (ii) as a foundation for interpreting the spectral fingerprints of other stars.

As such, the historical arc of UV astronomy is inseparable from the development of our understanding of stellar variability and transients. As instruments matured, so too did the ambition of the questions posed. By the 1980s and 1990s, attention had shifted from cataloguing spectral features to tracking how they varied in time: stellar flares on active dwarfs, mass-loss episodes from evolved giants, pulsation cycles in Cepheids and the early-time signatures of supernovae (SNe). The time-domain dimension of UV astronomy has always been technically challenging—short exposures, limited sensitivity and the need for rapid response—but it became increasingly central to the field's predominant research direction. Indeed, the same chromospheric (magnetic) resonance lines—Mg II, C II, Si IV and C IV—that trace plages (bright patches in the chromosphere) and prominences (magnetic filaments) on the Sun also flare dramatically in cool stars, thus forging a powerful link between local solar physics and the broader behaviour of stellar populations (Butler et al. 1988; Loyd and France 2014, see Sect. 5 for a discussion of UV solar and stellar flares).

The launch of the Hubble Space Telescope (*HST*) in April 1990—equipped with instruments such as the Goddard High Resolution Spectrograph (GHRS) and, later, the Space Telescope Imaging Spectrograph (STIS) and the Cosmic Origins Spectrograph (COS)—brought a new level of spectral precision to UV diagnostics. With the *HST*, it became possible to measure line profiles in exquisite detail and probe velocity fields, atmospheric turbulence and absorption structures in both stellar and interstellar contexts (e.g., Carpenter et al. 1995). Complementing *HST*'s near- and far-UV coverage, the Far Ultraviolet Spectroscopic Explorer (*FUSE*; 1999–2007) provided high-resolution ($R \equiv \frac{\lambda}{\Delta\lambda} \sim 20,000$) spectroscopy at wavelengths inaccessible to *HST*, particularly in the 905–1187 Å range. It enabled transformative studies of O VI, the hydrogen Lyman series and molecular hydrogen in hot stellar atmospheres and the interstellar medium (ISM; e.g., Moos et al. 2000; Sahnow et al. 2000). Together, these facilities redefined UV diagnostics across stellar and interstellar environments. *HST*'s UV instruments, in particular, were critical in capturing the brief, luminous UV flashes that mark the shock breakout (SBO) of core-collapse SNe (see Sect. 6),

as well as for mapping accretion phenomena in cataclysmic variables and young stellar objects. The temporal resolution and sensitivity now allowed transients to be caught in the act rather than inferred retrospectively.

At the same time, dedicated missions such as the GAlaxy Evolution eXplorer (*GALEX*, launched in April 2003; Simons et al. 2014; Bianchi et al. 2017) extended UV studies into the wide-field extragalactic domain, mapping star formation across nearby galaxies (although at low spatial resolution) and providing context for the stellar activity seen in the Milky Way (Martin et al. 2005). *GALEX* demonstrated the power of UV tracers on galactic scales, whereas smaller missions such as the Neil Gehrels Swift Observatory (*Swift*; Hagen et al. 2017b; Ludwig et al. 2026), with its UV/Optical Telescope (UVOT), kept time-domain monitoring of SNe and gamma-ray bursts firmly in view (Roming et al. 2005). Together, these observatories established a continuum of sorts, from the physics of stellar atmospheres to the demographics of galaxies.

From a theoretical perspective, UV diagnostics have always occupied a privileged place because they access physical regimes that are otherwise inaccessible. Chromospheric resonance lines form at temperatures where non-local thermodynamic equilibrium (non-LTE) conditions dominate, making them sensitive to departures from radiative equilibrium and to the influence of magnetic heating (Linsky and Ayres 1978; Rutten et al. 1991). Transition-region lines trace plasma at temperatures of approximately 10^{4-6} K, thus providing unique diagnostics of flare energetics and coronal heating processes (Sasso et al. 2015; Del Zanna and Mason 2018). At higher energies, UV continua and the effects of non-LTE line blanketing (the cumulative effect of many absorption lines in a star's spectrum on its emergent radiation) in hot stars shape both photospheric opacities and serve as key signatures of strong, radiatively driven winds (Castor et al. 1975; Hillier and Miller 1998; Sander 2023). In all these cases, the UV regime probes the boundaries—between photosphere and chromosphere, between steady outflow and eruptive mass loss, between quiescence and transient flares.

As the next sections explore in detail, the applications of UV tracers span an extraordinary range. For low-mass stars, they reveal the architecture of the stellar atmosphere from photosphere to corona, and they provide the best diagnostics of flare energetics and long-term activity cycles. For high-mass stars, they expose the unstable winds and their eventual demise as SNe, where the first photons to escape the envelope often appear in the UV. And beyond the Milky Way, UV spectroscopy and photometry offer the most direct probes of massive-star populations and star-formation histories, particularly in metal-poor environments such as those characteristic of our nearest neighbours, the Magellanic Clouds (see Sect. 7).

It is worth stressing that the transient and variable sky, now a dominant theme across modern astrophysics, has always had a natural affinity with UV diagnostics. The sudden heating of plasma, the emergence of shocks and the dispersal of circumstellar material are all processes that are observed most brightly at UV wavelengths. As new facilities emerge—both space-borne and ground-based proxies, such as near-UV imagers—the importance of UV tracers will only increase. They remain indispensable, not only because they provide unique diagnostics but also because they remind us that stellar activity and transients are not exotic outliers but rather the normal modes of a dynamic Universe.

1.2 The UV as a Diagnostic Regime

The UV domain contains numerous diagnostics of chromospheric, transition-region and coronal activity, including Mg II, C II, Si IV, C IV and N V. These lines probe plasma spanning temperatures from $\sim 10^4$ K to 10^5 K and provide sensitive tracers of magnetic heating,

mass motions and atmospheric structure. Their formation and diagnostic interpretation are discussed in detail in Sect. 2.

UV observations are particularly sensitive to variability and transient behaviour. Solar and stellar flares, for instance, release most of their radiative energy in the UV, including the extreme UV (Hawley and Pettersen 1991; Kowalski et al. 2019). Stellar flares represent one of the most dramatic manifestations of magnetic activity and are among the most important targets for UV observations. Their observational characteristics and physical interpretation are discussed in Sect. 4.

Although flare stars had long been recognised from ground-based optical surveys, particularly among dMe stars (flare-active M dwarfs) and BY Draconis (BY Dra)-type variables—cool, magnetically active M dwarfs whose optical spectra exhibit strong emission lines (Gershberg 1972)—the UV opened an entirely new window on their physics. *IUE* provided the first opportunity to monitor stellar flares spectroscopically at high cadence. Observations of active late-type dwarfs revealed abrupt and large-amplitude enhancements in chromospheric and transition-region lines (most notably Mg II h and k, C IV and Si IV), accompanied by a strong rise in UV continuum emission (Butler et al. 1981; Hawley and Pettersen 1991). These signatures demonstrated that flare heating can penetrate to atmospheric layers far above those accessible to optical diagnostics and that UV line intensities may exceed their quiescent levels by orders of magnitude. The simultaneous growth of optical Balmer and Ca II H and K emission with the UV continuum confirmed that the impulsive flare phase coincides with intense chromospheric heating and particle acceleration.

Subsequent space missions broadened both the scope and the diagnostic power of UV flare studies. *GALEX* extended the investigation to a wider range of spectral types, showing that impulsive UV brightenings are common across the main sequence rather than confined to classical flare stars (Welsh et al. 2007). *HST*'s STIS and COS enabled time-resolved spectroscopy of individual flare events, revealing that multiple plasma components contribute to the UV response and that post-flare cooling persists long after the impulsive phase (Loyd and France 2014). *Swift*, with its combined UV and X-ray sensitivity, has since provided a powerful means of correlating radiative outputs across bands, establishing the central role of magnetic reconnection (the process where magnetic-field lines snap and reconnect, releasing stored magnetic energy as heat, motion and energetic particles) in heating stellar coronae (Osten et al. 2016; Loyd et al. 2018a). Collectively, these developments have shown that flares dominate the short-term variability of late-type stars in the UV and contribute substantially to their cumulative magnetic energy budget. The resulting UV radiation environments have profound implications for planetary atmospheres and for interpreting variability in stellar populations observed in the integrated light of galaxies.

In high-mass stars, the UV regime probes different physics. The strong resonance lines of C IV, N V and Si IV reveal powerful stellar winds driven by line scattering of UV photons (Castor et al. 1975; Lamers and Cassinelli 1999). These winds influence stellar evolution, stripping mass and angular momentum and enriching the ISM with chemically processed material. The UV domain also captures the brief but luminous emission from SN SBOs. Models predict that the first light from core-collapse events emerges predominantly in the UV, with durations of minutes to hours (Matzner and McKee 1999; Waxman and Katz 2017). Detecting these UV flashes provides unique constraints on progenitor radii and circumstellar environments. The limited number of such detections to date underscores both the promise and the challenges of UV transient astronomy.

The reach of UV diagnostics extends well beyond the stars of our own Galaxy. In the Magellanic Clouds, where metallicities are well below solar, UV spectroscopy has been essential in testing how stellar winds depend on composition. Observations with the *HST*

and *FUSE* demonstrated that O-star winds in the Small Magellanic Cloud are weaker than their Galactic counterparts, consistent with the metallicity-dependent scaling predicted by line-driven wind theory (Mokiem et al. 2007). More broadly, the rest-frame UV has become the cornerstone of extragalactic star-formation studies, particularly at high redshifts where optical observations probe the far-UV of young galaxies. Templates derived from UV spectroscopy of stars and star clusters in the Magellanic Clouds remain critical for interpreting galaxy spectra in the early Universe (Leitherer et al. 1999, 2010; Chisholm et al. 2019; Senchyna et al. 2022, see also Subramaniam et al. 2026, this collection). Thus, UV diagnostics form a continuous bridge: from stellar activity in the Sun and nearby stars, through massive-star winds and transients, to galaxy-scale star formation across cosmic time.

1.3 The Modern Landscape of UV Astronomy

Nevertheless, UV astronomy remains resource-limited. The dependence on space-borne platforms has meant that UV facilities are relatively few compared with ground-based optical or radio telescopes. The *HST* continues to operate, but its eventual retirement is approaching rapidly. *GALEX* was decommissioned in 2013, and *FUSE* ceased operations in 2007. Yet the future seems promising. Dedicated missions such as *ULTRASAT*, scheduled for launch in the mid-2020s, promise to open the time-domain UV frontier with wide-field monitoring capable of capturing hundreds of early SN light curves each year (Shvartzvald et al. 2024). Proposed missions (for an extensive review, see Barstow et al. 2026, this collection) such as *Polstar*, designed to combine UV spectroscopy with spectropolarimetry, would bring magnetic-field diagnostics into the UV (Scowen et al. 2022). Meanwhile, multipurpose observatories like the James Webb Space Telescope (*JWST*), although lacking UV coverage, have reinforced the complementary role of the UV: *JWST*'s infrared view of galaxies and exoplanets makes UV stellar data even more valuable as a counterpart. The synergy between UV and other wavelengths will only deepen as astrophysics moves further into the era of multi-messenger and time-domain exploration.

Several cross-cutting themes emerge from this narrative. First, the UV range provides high contrast between quiescent and active states. Where photospheric radiation dominates the optical regime, magnetic heating and transient processes stand out in the UV. Second, the UV unifies diagnostics across mass and evolutionary stage: the same wavelength regime that traces chromospheric heating in M dwarfs also reveals line-driven winds in O stars and the SBO flashes of SNe. Third, UV studies are fundamentally time-domain in character. The most revealing signals—whether flares, shocks or transient luminosity increases—are inherently variable, demanding instruments with both sensitivity and cadence. Finally, the UV connects disciplines: stellar astrophysics, exoplanet science, galactic evolution and cosmology all depend, in different ways, on UV diagnostics.

This introductory review section sets the stage for the more detailed discussions to follow. In Sect. 2, we turn to the theoretical underpinnings of stellar chromospheric lines and explain why UV resonance transitions serve as privileged diagnostics of activity. Section 3 explores the lessons we can learn from variability studies of pre-main-sequence (PMS) stars. Section 4 surveys the observational landscape for low-mass FGKM-type stars, emphasising the chromospheric, transition-region and coronal layers. Section 5 focuses on UV flare diagnostics, whereas Sect. 6 explores the UV view of massive stars on the brink of explosion, focussing on progenitor models and the fleeting UV flashes of SBOs. Section 7 extends our scope to extragalactic environments, showing how UV diagnostics trace star formation in the Magellanic Clouds and—ultimately—provide templates for high-redshift galaxies. Together, these sections build a comprehensive picture of how UV observations reveal stellar activity and transients across the cosmos.

2 Stellar Activity in the UV: Theoretical Basis

In this section, we will address the following three key questions, with a focus on the chromosphere and the transition region:

1. What does 'stellar activity' mean in practice?
2. Why do UV lines trace stellar activity? and
3. How should we interpret key diagnostic lines tracing stellar activity?

2.1 What Is Stellar Activity and Why Does the UV Trace It?

Building on the overview presented in Sect. 1.2, we now examine the physical basis of UV activity diagnostics in greater detail. 'Stellar activity' is a catch-all term that refers to departures from purely radiative equilibrium and steady hydrostatic flows in the outer layers of stars. It includes additional heating, momentum input and time-dependent dynamics occurring above the photosphere. The region of stellar activity includes the chromosphere, the transition region, the corona and any connected in- or outflows. Phenomenologically, activity reveals itself through enhanced emission over and above the photospheric continua, variability from seconds to decades, broadened or asymmetric spectral features, quasi-periodic cycles and mass loss—ranging from transient ejections to steady winds. Physically, it is the conversion of mechanical, magnetic or gravitational energy into thermal energy, wave energy and bulk flows. On spatial scales, bulk flows range from flux-tube widths to stellar radii, and on temporal scales they cover the time span from Alfvén crossing times to magnetic and rotational cycles. Whereas magnetic fields are the dominant driver in many cool stars, stellar activity in a broader sense also includes pulsation-driven shocks, radiation-driven winds and accretion-powered phenomena.

A basal (quiescent) chromospheric flux persists even in very inactive stars and is commonly attributed to non-magnetic heating (Schröder et al. 2012). It is driven by convective acoustic waves that steepen into shocks in the quiet chromosphere, independent of rotation. The magnetic excess above this floor correlates with rotation through the Rossby number (Schrijver 1987), $Ro = P_{\rm rot}/\tau_{\rm conv}$, where $\tau_{\rm conv}$ is the convective turnover time—the characteristic timescale for a convective cell to rise to the surface—following the unsaturated Ro scaling and then saturating for $Ro \lesssim 0.1$ at a nearly constant activity level.

In stars with a convective envelope and a relatively low effective temperature, including FGKM-type stars, stellar activity is predominantly magnetic. The interplay of convection, rotation and magnetic fields generates large amounts of magnetic energy. This energy is transported to the stellar surface and into the atmosphere, where it dissipates through processes like magnetic reconnection and wave heating, the process by which mechanical and magnetic waves generated in the star's lower layers propagate upwards and deposit energy in the upper atmosphere. This non-radiative energy deposition heats the outer atmosphere to extreme temperatures. Above the photosphere, the chromosphere is characterised by an increasing temperature gradient and partial ionisation. It is followed by a narrow transition region at higher altitudes where the temperature and ionisation potential fraction rise steeply, leading into an overlying corona exhibiting high thermal and magnetic pressures.

In hotter stars with radiative envelopes, including early A-, B- and O-type stars, large-scale convective dynamos are weak or absent, and the dominant stellar activity arises from radiation forces, pulsation and accretion. Momentum is transferred from the stellar radiation field to the gas via metal-line opacity, in turn producing line-driven winds whose UV resonance profiles (e.g., N V, C IV, Si IV) show P Cygni shapes (reflecting strong outflows

or stellar winds), discrete absorption components and clumping signatures. In radially pulsating stars (e.g., Cepheids, RR Lyrae and Mira variables), periodic shocks steepen in the atmosphere and heat/accelerate material; in accreting systems (young stars and interacting binary systems), gravitational energy released in accretion funnels or at boundary layers powers hotspots and fast flows. However, across these cases the drivers differ: radiation pressure, global pulsation dynamics or gravitational potential energy all form part of what we call stellar activity.

Given this context, one might wonder why diagnostic lines at UV wavelengths are especially responsive to stellar activity. Spectroscopically speaking, a line is deemed 'diagnostic' when certain specific, measurable features (flux, flux ratio, width, shift, shape) map in a controlled fashion to a range of underlying plasma properties. The UV regime hosts a dense set of such probes that are selectively sensitive to the atmospheric layers where stellar activity originates.

Specific UV diagnostic lines are tuned to the thermodynamic regime where stellar activity is generated. A star's stratified outer atmosphere runs from the upper photosphere ($\sim 6 \times 10^3$ K) through the chromosphere and into the transition region, where the plasma is heated rapidly to $\sim 10^{5-5.5}$ K before it continues to feed the higher-level coronal plasma at $\gtrsim 10^6$ K.[1] Many strong UV resonance lines arise from ions whose ionisation fractions and contribution functions peak in this temperature range, e.g., Si IV ($\log T$ [K] $\approx$ 4.9), C IV ($\log T$ [K] $\approx$ 5.0) and N V ($\log T$ [K] $\approx$ 5.3).[2] As such, any process that perturbs the heating rate, the pressure or the flows in these layers (magnetic reconnection, wave dissipation, pulsation shocks, line-driven instabilities, accretion impacts) directly changes the ionisation-level populations and emissivities of the UV transitions. Because the optical/near-UV photospheric continuum of cool stars is relatively bright, whereas the far-UV continuum is generally weak, the UV line-to-continuum contrast is high, thus rendering modest physical changes spectroscopically conspicuous.

Radiatively speaking, UV line formation is highly non-local and therefore very sensitive to activity. Densities in the chromosphere and transition region are low enough that collisional de-excitation rates are often small compared to radiative decay, so the line source function S_ν is dominated by scattering, i.e. $S_\nu \simeq (1-\epsilon)\, J_\nu + \epsilon\, B_\nu$, with the photon destruction probability $\epsilon \ll 1$ and B_ν representing the Planck blackbody function (thermal emission). In this regime, the angularly averaged radiation field J_ν, which carries information from neighbouring altitudes and structures, controls the emergent intensity. Thus, modest perturbations in temperature, density or velocity along the line of sight can imprint outsized changes onto UV line cores and wings. Line cores form at higher altitudes within the stellar atmosphere, where the optical depth is large, and respond to overlying cool/hot layers and flows; line wings originate deeper into the stellar atmosphere and track gradients and micro-turbulence. For a few resonance lines (Lyα, Mg II h and k), line wings also track partial frequency redistribution (PRD) physics, which describes how the frequency of a photon changes when it is absorbed and re-emitted.

Kinematically speaking, UV lines offer clean, fast probes of dynamics occurring on activity timescales. Their large oscillator strengths and short radiative lifetimes produce sharp, high-contrast profiles with Doppler shifts of a few km s^{-1} in the quiescent transition region (Chen et al. 2022) to hundreds of km s^{-1} in winds, accretion events and flares (Prinja

[1] Canonical temperature structure from semi-empirical solar models (Vernazza et al. 1981; Fontenla et al. 2009); coronal temperatures summarised by Reale (2014).

[2] Peak formation conditions (optically thin, ionisation equilibrium) from the CHIANTI database (Young et al. 2016; Dere et al. 2019; Del Zanna et al. 2021).

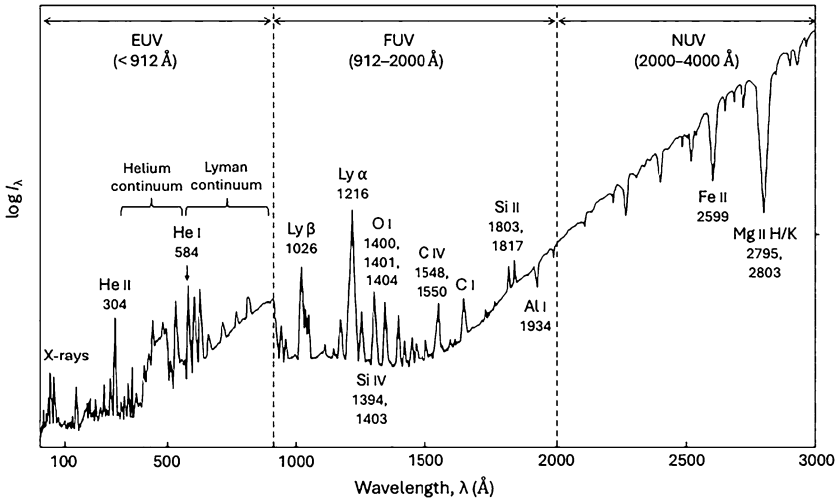


Fig. 1 Schematic rendition of the UV solar spectrum. EUV, FUV, NUV: Extreme, far- and near-UV. (After Rob Rutten's lecture notes; http://www.staff.science.uu.nl/~rutte101/rrweb/rjr-edu/lectures/rutten_ssx_lec.pdf)

et al. 1990). Bulk flows associated with chromospheric evaporation/condensation, pulsation-driven shocks, accretion funnels or wind acceleration appear as asymmetric wings, centroid shifts or P Cygni-type morphologies. Non-thermal broadening (from waves and turbulence) adds to thermal line widths and grows with formation temperature, thus enabling a temperature-ordered view of unresolved motions from the chromosphere to the transition region.

These attributes, including layer selectivity, high contrast in cool-star spectra, rapid time response and a rich menu of line ratios, turn UV lines into *bona fide* diagnostics of stellar activity.

2.2 How Should We Interpret Key Diagnostic Lines Tracing Stellar Activity?

We now provide a practical summary list of the key UV diagnostic lines. Refer to Fig. 1 for a schematic overview of a selection of these lines.

- Mg II *h* (2803.53 Å) – *Region:* upper photosphere → chromosphere; *Blends/notes:* Fe I/II nearby, PRD; *Caveats:* Mg II h/k deviates from a 2:1 ratio owing to opacity/PRD.
- Mg II *k* (2796.35 Å) – *Region:* upper photosphere → chromosphere; *Blends/notes:* Fe I/II nearby, PRD; *Caveats:* strong opacity, core reversal (when the centre of an emission line is less intense than its wings, producing a dip at the line core), possible ISM absorption.
- C III (1906.68, 1908.73 Å) – *Region:* transition region; *Blends/notes:* Fe III/Si III; *Caveats:* requires near-UV coverage, higher extinction, useful for n_e (electron density) diagnostics.
- He II (1640.40 Å) – *Region:* photoionisation/recombination; *Blends/notes:* Fe II multiplets; *Caveats:* traces extreme-UV/X-rays, not a simple temperature diagnostic.
- C IV (1548.20, 1550.77 Å) – *Region:* mid-transition region; *Blends/notes:* Fe II/Si I in cool stars; *Caveats:* strong non-thermal wings.
- O IV (1399.77, 1401.16, 1404.78 Å) – *Region:* transition region; *Blends/notes:* the line at 1404.78 Å is blended with Si IV; *Caveats:* de-blend carefully, useful for n_e diagnostics.

- Si IV (1393.76, 1402.77 Å) – *Region:* mid-transition region; *Blends/notes:* inter-system blends, narrow ISM lines; *Caveats:* doublet ratio < 2 indicates opacity/scattering.
- C II (1334.53, 1335.71 Å) – *Region:* lower transition region; *Blends/notes:* H_2/ISM blend; *Caveats:* often optically thick in active stars.
- N V (1238.82, 1242.80 Å) – *Region:* hot transition region; *Blends/notes:* near Lyα wings; *Caveats:* faint in old/inactive stars.

This compact list contains the most frequently used UV diagnostics and their associated caveats. In practice, interpretation benefits from separating

(i) regions where a line forms;

(ii) how it forms (optically thick non-LTE with scattering versus optically thin collisional/radiative);

(iii) which plasma property it primarily constrains (heating, density, kinematics).

Below, we outline a mechanism-agnostic reading of the diagnostics.

1. *Chromospheric resonance lines (Mg II h and k).*

Mg II *h* and *k* form across the upper photosphere and chromosphere in strong resonance scattering with PRD. The wings sample the deeper, warmer atmospheric layers and reflect the local temperature gradient and microturbulence; the line cores form in the higher, scattering-dominated layers ($\epsilon \ll 1$). They often show central reversals caused by overlying cooler layers and flows (Leenaarts et al. 2013a,b). Core asymmetries (red or blue) of Mg II *h* and *k* are good tracers of bulk motions, whereas time variability encodes impulsive heating and subsequent relaxation. Because the opacity is high, profiles must be modelled with non-LTE radiative transfer.

2. *Transition-region resonance doublets (C IV, Si IV, N V).*

These lines are often well-described as optically thin collisional lines, with radiative emitters in plasma near their formation temperatures ($\log T$ [K] ≈ 4.9–5.3). Their integrated fluxes scale with the emission measure at $\sim 10^5$ K (Dere et al. 2019; Del Zanna et al. 2021), thus enabling constraints on both heating and the differential (temperature-dependent) emission measure. They are prime tracers of chromospheric evaporation and turbulent broadening; line widths generally grow with increasing formation temperature. In very active stars, doublet ratios <2 reveal opacity and scattering.

3. *He II 1640 Å as an extreme-UV proxy.*

He II 1640 Å is mainly powered by photoionisation/recombination and, thus, responds to the unobserved extreme-UV/X-ray radiation field as well as to transition-region conditions. Its strength, combined with a resonance-line tracer (e.g., C IV), can be used to reconstruct the stellar extreme-UV budget relevant to atmospheric escape and photochemistry in exoplanetary systems (France et al. 2018). Because it is not a single-temperature diagnostic, it should be interpreted within a multi-line context.

In summary, stellar activity encompasses the suite of processes that add non-radiative energy and momentum to the outer atmosphere. It builds chromospheres, transition regions and coronae and drives in- and outflows. In cool stars, it is chiefly magnetic; in hot stars, it originates from radiation forces, pulsation and accretion. Observationally, stellar activity appears in the form of excess line emission, profile asymmetries/broadening and variability across a wide range of timescales. UV lines trace this activity, because their strongest transitions form where the energy is actually deposited—that is, between the upper chromosphere and the transition region—under low densities that make formation highly non-local

and sensitive to small perturbations. The associated high line-to-continuum contrast and advances in photon-counting time resolution turn modest changes in heating and flows into useful diagnostic spectroscopic signals.

3 UV Spectroscopy of Pre-Main-Sequence Stars

PMS stars are significantly brighter in the UV than their main-sequence descendants, largely owing to their larger radii, ongoing gravitational contraction and enhanced activity (accretion and shocks). At early evolutionary stages, their UV luminosities can reach up to $0.2 L_{\odot}$, particularly when accretion and bipolar outflows begin to disperse the surrounding cocoon of gas and dust. The UV diagnostics of PMS stars depend strongly on stellar mass and evolutionary stage. In particular, the spectral tracers observed in low-mass T Tauri stars (TTSs; $M \leq 2 M_{\odot}$) differ from those characteristic of the more massive Herbig Ae/Be (HAeBe) stars. The main spectroscopic differences from their main-sequence analogues arise from the contribution by powerful outflows and accretion discs.

3.1 Low-Mass PMS Stars

TTSs become detectable at UV wavelengths typically at ages of ~ 1 Myr. Their strong UV emission is primarily driven by accretion (Ingleby et al. 2013; Hartmann et al. 2016), with gravitational energy being released in the form of shock fronts at the stellar surface. Although the UV luminosity declines as the star approaches the main sequence, even at ages of ~ 100 Myr, low-mass PMS stars still display spectral features characteristic of highly active stars, similar to those of the M-type emission-line (dMe/Me) stars.

The UV spectra of low-mass PMS stars share spectral diagnostics with magnetically active stars (see Sect. 2). The surface fluxes of these lines are typically 10^{6-7} erg cm^{-2} s^{-1}, approximately 2 orders of magnitude higher than those observed in the Sun (Imhoff and Giampapa 1980; Lemmens et al. 1992; Gómez de Castro et al. 1997). The distinct characteristics of PMS stars become especially evident when compared with their main-sequence counterparts. As illustrated in the standard flux–flux diagrams (see, e.g., Figs. 2 and 3) used to study energy transport in the atmospheres of cool stars, there is notable excess emission of singly ionised species which is not caused by metallicity effects (all TTSs are members of the Taurus–Auriga star-forming region). High-resolution spectroscopic studies have measured a mean iron abundance close to solar, [Fe/H] $\simeq 0.0$ dex, with only a small star-to-star dispersion. This suggests that the Taurus population is chemically homogeneous and does not contain a significant metal-rich component (D'Orazi et al. 2011). This emission originates from an extended plasma region surrounding the star, which is not directly heated by collisional processes or by photoionisation from the stellar surface. Part of this excess is attributed to unresolved outflows, whereas another portion is thought to arise from the star's extended magnetosphere—an area that can span several stellar radii and channels accretion flows onto the stellar surface. In this sense, a notable feature is the distinct relationship between X-ray and He II emission and the relatively high X-ray luminosity in PMS stars compared with their main-sequence counterparts, reflecting differences in magnetic activity, accretion processes and energy-dissipation mechanisms during the PMS phase.

Flux–flux relations are powerful diagnostics for disentangling the relative contributions of accretion and other heating processes. This was demonstrated through the monitoring of the PMS binary AK Scorpii (AK Sco), a close binary system surrounded by a circumbinary

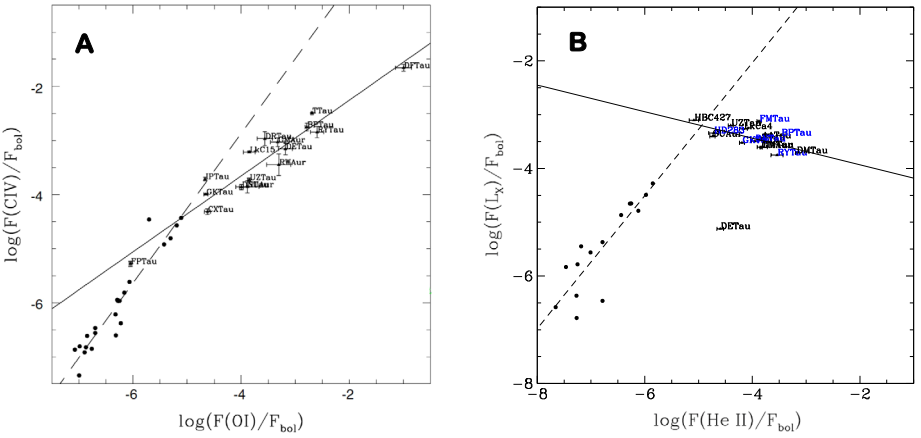


Fig. 2 (A) Comparison of the C IV to O I flux ratios of TTSs and main-sequence stars. (B) Comparison of the X-ray to He II flux ratios of TTSs and main-sequence stars. The main-sequence UV fluxes are from Ayres et al. (1995) for G0 to K4 types and from Linsky et al. (1982) for K5 to M5.6 types. (Credit: Gómez de Castro and Marcos-Arenal 2012)

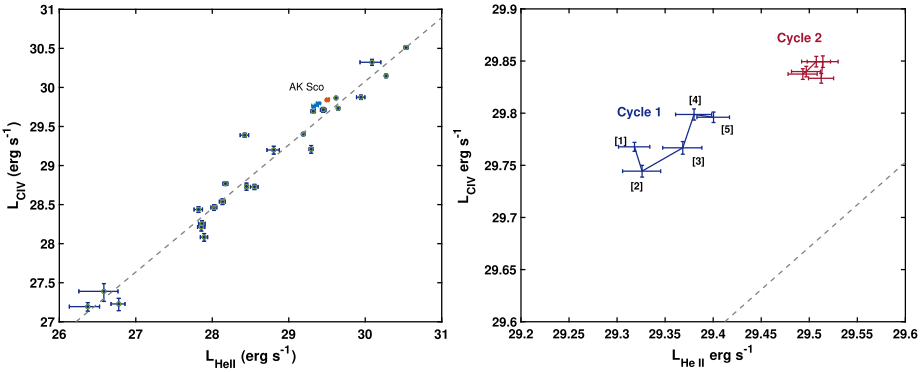


Fig. 3 C IV–He II flux–flux diagrams. (left) All TTSs were observed with the *HST*, using the same configuration (STIS/G140L). AK Sco observations are shown in blue (Cycle 1) and red (Cycle 2). The best-fitting regression line is also included. (right) Enlargement of the location of AK Sco observations. The order of the observations in Cycle 1 is marked by [1], [2], . . . ; 1σ error bars are shown (Gómez de Castro et al. 2020)

disc, where the strongest accretion events occur near periastron. Observations obtained during two consecutive periastron passages follow distinct tracks in the flux–flux diagrams, a behaviour interpreted as evidence that the relative importance of accretion with respect to other heating mechanisms varies from epoch to epoch (Gómez de Castro et al. 2020).

Another significant spectroscopic characteristic is the occurrence of prominent Fe II emission. Many multiplets are observed, including UV 2, 3, 35, 36 (2330–2410 Å); UV 32, 62, 63 (2700–2750 Å); and UV 60, 78 (2900–3000 Å) (Gahm et al. 1979; Brown et al. 1984; Gómez de Castro et al. 1997). Although the Fe II lines are individually weaker than the equivalent Mg II, C II or Si II lines, they are so numerous that their combination becomes a significant coolant of the PMS stellar atmospheres (see, e.g., Jordan and Kuin 1988). The excitation mechanism of the transitions is not purely collisional; recombination following

photoionisation is also an important pumping route that is especially significant for transitions pumped by Lyα photons—such as the Fe II transition at 2507 Å. The latter account for as much as 80 per cent of the total far-UV flux of TTSs.

The spectral lines display significant supra-thermal broadening which decreases as the stars evolve towards the main sequence (Ardila et al. 2013; Gómez de Castro 2013). This broadening is often interpreted as comprising two components, including a broad component associated with magnetospheric accretion and a narrow component likely originating from the heated stellar atmosphere. As the TTSs approach the main sequence, the broadening decreases until it reaches the thermal broadening observed in main-sequence stars

Intercombination (semi-forbidden) transitions are also observed in many spectra. In some cases they are produced in unresolved jets (Gómez de Castro and Verdugo 2001; López-Martínez and Gómez de Castro 2014), but they mostly originate from extended magnetospheric structures located between the star and the inner boundary of the accretion disc—such as the ion torus detected in RW Aurigae (RW Aur) (Gómez de Castro and Verdugo 2003). The C III, Si III] and O III] transitions have also been used as diagnostic tools to probe accretion shocks (Gómez de Castro and Lamzin 1999). The strongest transitions are:

- C II] 2324.21, 2325.40, 2326.11, 2327.64 and 2328.84 Å [$2s^2 2p\ (^2P^0) \rightarrow 2s2p^2\ (^4P)$];
- Si II] 2328.52 and 2334.41 Å [$3s^2 3p\ (^2P^0) \rightarrow 3s3p^2\ (^4P)$];
- C III] 1908.73 Å [$2s^2\ (^1S) \rightarrow 2s2p\ (^3P^0)$];
- Si III] 1892.03 Å [$3s^2\ (^1S) \rightarrow 3s3p\ (^3P^0)$]; and
- O III] 1660.81 and 1666.15 Å [$2s^2 2p^2\ (^3P) \rightarrow 2s2p^3\ (^5S^0)$].

Figure 4 shows example C II] and Si II] profiles; the contribution of Fe II] transitions is also detected [$3d^6 4s\ (5D) \rightarrow 3d64p(5D)$]. From careful analysis of such profiles, important information about the prevailing magnetospheric plasma properties in the magnetospheric flow can be measured, such as the electron temperatures ($10^{4.1-4.5}$ K) and the range of electron densities, spanning from 10^8 cm^{-3} to 10^{12} cm^{-3}. The line widths are supra-thermal, and the broadening correlates with the accretion rate; only two TTSs displayed thermal broadenings, including CY Tauri (CY Tau) and, more interestingly, TW Hydrae (TW Hya; shown in Fig. 4). In a few stars the line centroids are blue-shifted, indicating that the line emission is dominated by outflows.

The molecular gas in circumstellar discs also produces notable signatures in UV spectra (Herczeg et al. 2002, 2004; France et al. 2012b; McJunkin et al. 2013). The most abundant molecules, H_2 and CO, exhibit strong electronic transitions that are pumped by Lyα photons. In particular, the transitions from the ground state ($X^1\Sigma_g^+$) to low-lying excited states—Lyman ($2p\sigma$, $B^1\Sigma_u^+$) (Abgrall et al. 1993a) or Werner ($2p\pi$, $C^1\Pi_u$) (Abgrall et al. 1993b) levels, i.e. the two primary electronic excited-state systems of molecular hydrogen, H_2, that produce the characteristic far-UV absorption and emission bands. The CO transitions are also pumped by Lyα photons by means of several rotational transitions of the $A^1\Pi \rightarrow X^1\Sigma^+$ (fourth positive) electronic system.

Beyond the emission-line diagnostics discussed above, the UV continuum itself provides a valuable probe of PMS evolution. Classical TTSs frequently exhibit a pronounced UV excess relative to the photospheric continuum expected for a main-sequence star of the same spectral type. This excess is generally attributed to hot accretion shocks formed where magnetically channelled material impacts the stellar surface, producing continuum emission that can dominate the near-UV spectrum. Measurements of this UV excess are widely used to estimate accretion luminosities and mass-accretion rates. In contrast, weak-lined TTSs typically show continua much closer to photospheric expectations, with chromospheric activity contributing primarily through line emission rather than a strong continuum excess (Calvet

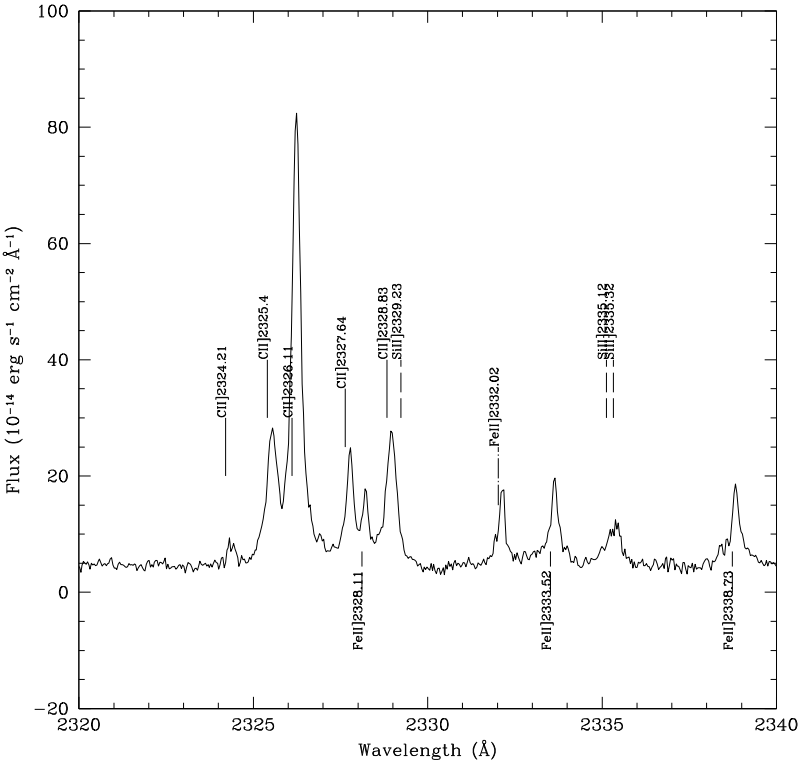


Fig. 4 The C II], Fe II] and Si II] blend observed in TW Hya. The line broadening in this spectrum is thermal, and the individual features are well-resolved (López-Martínez and Gómez de Castro 2014)

and Gullbring 1998; Gullbring et al. 1998; Ingleby et al. 2013). The UV continuum of TTSs generally declines with age as accretion rates decrease, evolving from the strong accretion-driven UV excesses observed in classical TTSs to the weaker, predominantly chromospheric emission characteristic of weak-line TTSs (see Gómez de Castro et al. 2026, this collection).

3.2 Herbig Ae, Be Stars

HAeBe stars are intermediate-mass (2–10$M_{\odot}$) PMS stars, whose formative processes and outer atmospheres remain the subject of ongoing research. Although their relatively high masses suggest that their gravitational collapse should be super-Alfvénic—thus rendering magnetic fields a minor driver—accumulated observations imply a more nuanced view. Their UV emission-line spectra indicate the presence of a chromosphere above the photosphere (Deleuil et al. 2005), and the detection of highly ionised species (transition-region or corona-like), together with the detection of weak magnetic fields (Donati et al. 1997; Järvinen et al. 2019), implies that magnetic drivers are indeed active during at least the first $\sim 5 \times 10^6$ yr of PMS evolution. They remain rather puzzling objects.

Monitoring campaigns in the UV and optical ranges first revealed azimuthal structures in the wind of AB Aurigae (AB Aur; Praderie et al. 1986). Subsequent extensive spectroscopic monitoring (e.g., the MUSICOS campaigns; Catala 1998) revealed that chromospheric structures rotate with a period of 32 hours (consistent with the stellar rotation period), whereas

the wind (traced by UV Mg II lines) exhibits a longer, 45 hour period (Boehm et al. 1996; Catala et al. 1999). UV studies have also identified clumps of very hot gas in the AB Aur wind, traced by N V emission (Bouret et al. 1997). These features strongly suggest a multi-component wind structure, which can be described as follows:

- A 'slow' dense outflow, attaining terminal velocities of ~ 300 km s^{-1}, responsible for the prominent P Cygni profiles in Ca II and Mg II uv1 lines (the strongest resonance transitions of a singly ionised metal in the UV) and the broad blue-shifted absorption seen in C IV. Semi-empirical modelling allows inference of mass-loss rates of order $10^{-8} M_{\odot}$ yr^{-1} (Catala and Kunasz 1987; Bouret and Catala 1998).
- A 'high-velocity' component, composed of magnetically confined streamers forming a faster outflow. Because HAeBe stars are rapid rotators, gas in the streamers is forced into co-rotation out to the Alfvén radius, the distance where the stellar-wind speed equals the Alfvén speed. This leads to shocks between the slow and fast wind components and the formation of dense azimuthal structures at co-rotating interaction regions.

Magnetically confined flows are further supported by detections of Lyα emission from the jets associated with the HAeBe stars HD 163296 and HD 104237 (Devine et al. 2000; Grady et al. 2004). Moreover, magnetic dissipation provides a plausible mechanism for the radiative losses observed in the chromosphere and wind of about 4–8 per cent of the stellar bolometric luminosity (Bouret and Catala 1998), but accretion streams may also contribute (Blondel et al. 1993; Bouret and Catala 2000; Roberge et al. 2001). Although accretion likely does not drive the bulk of the outflow, radiatively driven winds can become collimated in the presence of a modest magnetic field (Sakurai 1985; Rotstein and Gimenez de Castro 1996). The origin of the magnetic field remains an open question; possibilities include a dynamo operating in the outer stellar layers, with turbulence induced by pulsations—radial and non-radial, with periods from tens of minutes to hours (see Catala 2003)—or by shear generated through rotational wind braking (Lignieres et al. 1996).

Recent UV spectroscopic investigations have provided deeper insights. High-resolution UV spectra of a small HAeBe sample show that the luminosity of the C IV doublet scales (albeit with scatter) with the estimated accretion rate, thus extending trends found for lower-mass stars. Nevertheless, the line shapes are consistent with optically thin winds rather than magnetospheric accretion flows (Cauley and Johns-Krull 2016). Mid-infrared forbidden-line studies (e.g., [Ne II] and [Ne III]) also suggest that high-energy irradiation (UV, extreme-UV, X-rays) plays a key role in shaping the circumstellar environments of HAeBe stars (Akhila et al. 2025).

Combined, these results support a paradigm where HAeBe stars, despite their higher masses and more rapid evolution, host structured chromospheres and magnetically mediated winds that bear both similarities to and distinctions from the lower-mass T Tauri class. The extant evidence emphasises that magnetic fields, although perhaps weaker or more complex, remain important during the early phases of intermediate-mass PMS evolution; that hot plasma and structured winds are significant; and that UV emission lines remain a powerful diagnostic of the outer stellar environment and its dynamics. Future progress will benefit from high-resolution UV spectroscopy and coordinated multi-wavelength campaigns in the intermediate-mass regime.

4 Low-Mass Stars in the UV: Observational Status

Cool stars with convective envelopes—particularly those of spectral type F and later—exhibit magnetic activity throughout their atmospheres. In the Sun, where we can resolve

surface features, activity features manifest as large, rapidly evolving starspots and faculae in the photosphere, prominences and filaments in the chromosphere, and energetic flares or coronal mass ejections (CMEs) from the corona (e.g., Berdyugina 2005; Brun et al. 2015; de Grijs and Kamath 2021). Multiwavelength diagnostics, including photometric variability tracing photospheric activity, chromospheric emission lines such as Ca II H and K, Hα and Mg II, as well as UV/X-ray flux measurements from the corona, provide a comprehensive framework for probing the generation and evolution of these phenomena. Low-mass stars display varying levels of magnetic activity over their lifetimes, thus making it essential to understand how evolutionary processes shape these changes. Key open questions include how stellar rotation spins down with time, how magnetic activity evolves with age and which fundamental parameters govern these relationships. To date, most studies have concentrated on studying individual activity indicators, often limited by observational constraints. However, the advent of large-scale time-domain surveys now offers unprecedented opportunities to investigate magnetic activity across multiple wavelengths, particularly in the optical and UV domains.

Optical and near-UV emission originates from the cool ($T \approx 10^4$ K), lower stellar atmosphere, whereas far-UV lines trace the hotter ($T \approx 10^5$ K) transition-region plasma (Kowalski 2024b). Owing to this sensitivity to hot plasma, the UV regime serves as a key diagnostic of stellar magnetic activity. The first extensive observations of chromospheric emission were obtained by *IUE*. Essentially all solar-type stars showed the presence of a chromosphere (traced by the line emission of, e.g., the Mg II doublet at 2800 Å, the C IV doublet at 1550 Å, Si IV at 1394 Å and many other, mostly weaker, lines). Giampapa et al. (1981) reported strong emission features in cool dwarfs, whereas Hartmann et al. (1979) and Haisch et al. (1980) identified intense flare-driven enhancements in stars such as Proxima Centauri (α Centauri C/α Cen C) and EQ Pegasi (EQ Peg). Butler et al. (1981) further showed that active M dwarfs (e.g., Gl 867 A and AU Microscopii/AU Mic) exhibit prominent UV emission lines, indicative of magnetically heated atmospheres.

GALEX enabled population-wide studies of stellar UV emission in both near-UV (1771–2831 Å) and far-UV (1344–1768 Å) bands (note that these definitions of the near- and far-UV are *GALEX*-specific), covering key diagnostic lines such as C II, C IV, Mg II and Fe II. *GALEX* also opened the time-domain frontier, revealing variability in M-dwarf flares (Welsh et al. 2007) and RR Lyrae pulsations (Wheatley et al. 2005). More recently, Bai et al. (2018) studied optical activity from the Large Sky Area Multi-Object Fiber Spectroscopic Telescope (LAMOST), combined with UV behaviour from *GALEX*, providing a statistical bridge between optical and UV diagnostics tracing magnetic activity.

UV flux measurements have long been central to understanding stellar activity and its influence on planetary atmospheres. UV radiation drives key photochemical reactions, including ozone formation and molecular dissociation, thus shaping planetary habitability (Miguel and Kaltenegger 2014; Harman et al. 2015). Whereas excessive near-UV flux can destroy biomolecules and O_3 (Rugheimer et al. 2015), moderate UV levels enable prebiotic chemistry (Rimmer et al. 2018; Ranjan et al. 2020). Recent studies have revealed that even optically inactive cool stars exhibit strong UV variability, often linked to flares (France et al. 2018; Loyd et al. 2018b; Jackman et al. 2023), yet long-term UV monitoring remains limited. Future dedicated UV missions are essential to trace stellar activity cycles, age–activity relations and the evolving radiation environments of exoplanet-hosting stars.

4.1 Active Variables Catalogue

In the past decade, photometric time-series surveys from space (*CoRoT*, *Kepler*, *K2*, *TESS*) and ground-based telescopes (OGLE, the Optical Gravitational Lensing Experiment;

Table 1 Catalogue of rotational variables detected from space-borne and ground-based time-series observations

Space-borne	
TESS (Fetherolf et al. 2023)	68,497
Kepler (Nielsen et al. 2013; McQuillan et al. 2014; Reinhold et al. 2023)	12,253; 34,030; 20,397
K2 (Armstrong et al. 2015; Reinhold and Hekker 2020)	9399; 32,387
Gaia (Distefano et al. 2023)	474,026
Ground-based	
OGLE (Iwanek et al. 2024)	18,443
ZTF (Chen et al. 2020; Chahal et al. 2022; Lu et al. 2022)	81,393; 40,553
ASAS-SN (Jayasinghe et al. 2020)	81,393

ASAS-SN, the All-Sky Automated Survey for SuperNovae; ZTF, the Zwicky Transient Facilty) have provided an extensive catalogue of variable stars. Most low-mass stars exhibit starspot/faculae modulation in their light curves, which is quasi-periodic in nature owing to the redistribution/evolution of spots and faculae. The availability of long-term, high-cadence observations for millions of stars has enabled the detection of rotational modulation in large samples of low-mass stars, as summarised in Table 1. These catalogues present a unique opportunity to exploit multiwavelength analysis (from the photosphere to the corona) to constrain the evolution of stellar activity across the low-mass stellar regime. However, comparatively fewer time-series observations have been obtained in the UV (e.g., *GALEX*) and in X-rays (*eROSITA*, *Chandra*, *NICER*). Upcoming UV missions (see Sect. 1.3 and Barstow et al. 2026, this collection) will enable comprehensive optical–UV time-domain studies of these rotational variables, allowing detailed characterisation of the flare properties, activity cycles and related phenomena discussed below. These observations will, in turn, provide statistical constraints on the generation and evolution of stellar magnetic activity in low-mass stars.

4.1.1 Flares from the Optical to the UV

Stellar flares are impulsive releases of magnetic energy that produce broadband photon emission from gamma-rays to radio wavelengths, with UV and optical bands exhibiting strong line emission and continuum fluxes that jointly dominate the radiative energy budget (Osten et al. 2005; Fuhrmeister et al. 2008). Observations from the HAZMAT programme (Shkolnik and Barman 2014) and the MUSCLES survey (France et al. 2016; Youngblood et al. 2017) revealed that the quiescent (basal) far-UV/near-UV luminosity increases by nearly 2 orders of magnitude from early-K to late-M dwarfs, and even optically inactive M dwarfs display frequent UV flares, as inferred from Hα and Ca II variability (France et al. 2013; Loyd et al. 2018b; Diamond-Lowe et al. 2021; Feinstein et al. 2022). Brasseur et al. (2023) identified numerous short-duration near-UV flares in *GALEX* and *Kepler* data (Martin et al. 2005; Borucki et al. 2010). Most lacked optical counterparts, thus demonstrating that rapid UV-bright flares are often missed in low-cadence optical observations. Coordinated high-cadence optical monitoring combined with rapid-response UV observations (e.g., with the *HST* or *Swift*) is therefore essential to capture the impulsive flare phases and construct contemporaneous optical–UV light curves. The large catalogue of rotational variables listed in Table 1 offers an opportunity to investigate flare properties across a broad range of stellar

masses and ages, emphasising the need for multiwavelength, high-cadence monitoring—particularly from the optical to the UV—to fully characterise stellar flare energetics. A more detailed discussion on stellar flares is presented in Sect. 5.

4.1.2 Stellar Activity Cycles

Stellar magnetic activity often exhibits cyclic variations driven by the underlying dynamo processes, exemplified by the 11-year solar cycle (Baliunas et al. 1995; Dikpati and Gilman 2006; Charbonneau 2020; de Grijs and Kamath 2021). Such cyclic behaviour has been studied extensively across a broad range of low-mass stars (Wilson 1968, 1978; Noyes et al. 1984; Baliunas et al. 1995; Brandenburg et al. 1998; Saar and Brandenburg 1999; Oláh et al. 2016; Reinhold et al. 2017; Boro Saikia et al. 2018; Olspert et al. 2018; Isaacson et al. 2024; Chahal et al. 2025). Nevertheless, the mechanisms governing the generation and evolution of stellar activity cycles remain poorly constrained, even for the Sun and Sun-like stars. Activity cycles are expected to depend sensitively on stellar rotation, mass, metallicity and other fundamental stellar parameters. Multiwavelength observations are essential to probe these cycles in detail. For instance, Wargelin et al. (2017) studied α Cen C's activity cycles across optical, UV and X-ray bands. A major challenge in detecting solar-like cycles is the limited time coverage of existing data sets. Recent work by Chahal et al. (2025) combined photometry from *Kepler* Full-Frame Images (Montet et al. 2017), ASAS-SN and ZTF, thereby enabling the detection of longer-term cycles. Additionally, ASAS-SN alone (Irving et al. 2023) also provides a valuable long-baseline data set. These extensive photometric surveys allow the construction of a large sample of rotationally modulated activity cycles (see Table 1), which can be followed up in the UV and at X-rays to probe multiwavelength activity tracers. Such studies offer critical insights into solar and stellar dynamos and can inform our understanding of habitable environments around other stars.

4.2 Correlation of Activity with Rossby Number

The stellar dynamo responsible for magnetic activity can be indirectly probed through the correlation between coronal emission and stellar rotation. This relation is commonly expressed in terms of the X-ray luminosity (L_X) or the UV flux as a function of the Rossby number and is inherently model-dependent. The X-ray activity–Rossby number relation exhibits two regimes, a saturated regime for rapid rotators and an unsaturated regime for more slowly rotating stars. Early X-ray and chromospheric studies already demonstrated the tight connection between rotation, Rossby number, and magnetic activity (e.g., Pallavicini et al. 1981; Noyes et al. 1984; Vilhu 1984; Stepien 1994). Pizzolato et al. (2003) later formalised this framework using a large, homogeneous *ROSAT* sample, clearly delineating the saturated and unsaturated regimes, and subsequent work (e.g., Wright et al. 2011; Stelzer et al. 2013, 2016; Wright and Drake 2016; Astudillo-Defru et al. 2017; Houdebine et al. 2017; Newton et al. 2017; Shulyak et al. 2017; Wright et al. 2018; Magaudda et al. 2020) has further refined the empirical picture.

While correlations between stellar activity and rotation have been studied extensively in X-ray and optical bands, relatively few authors have examined the corresponding trends in the UV regime (e.g., Vardavas 2005; Pineda et al. 2021). The Far Ultraviolet M-dwarf Evolution Survey (FUMES) (Pineda et al. 2021; Youngblood et al. 2021; Duvvuri et al. 2023, 2025) recently advanced this field by investigating UV emission, flare properties and their dependence on rotation for M dwarfs. Building on this progress, Chahal et al. (2023) analysed the chromospheric activity of ~16,000 low-mass stars as a function of rotation period

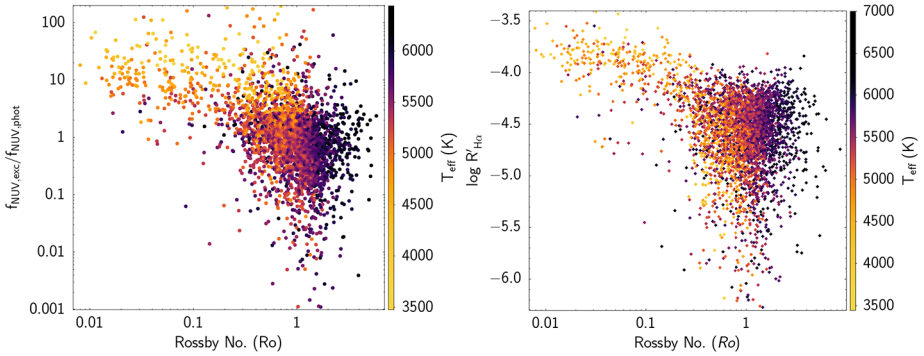


Fig. 5 Rossby number ($\equiv P_{\rm rot}/\tau_{\rm conv}$) plotted against (left) the fractional UV excess and (right) Hα activity indices. UV-excess values were derived from *GALEX* photometry (after Bai et al. 2018; Li et al. 2024), and the Hα indices were measured from LAMOST spectra (both from Chahal et al. 2023). The colour markers represent the stellar effective temperature, as indicated by the colour scale

and Rossby number (see Fig. 5, right). Figure 5 presents the fractional near-UV flux excess (left) derived from *GALEX* data (following Bai et al. 2018; Li et al. 2024) and the Hα-based chromospheric activity (right) as functions of the Rossby number, where $\tau_{\rm conv}$ was estimated using the empirical relation from Cranmer and Saar (2011). Both indicators exhibit a saturated regime at low Rossby numbers, transitioning to an unsaturated regime as the Rossby number increases; however, the latter does not display the same linear decline in activity typically observed in the X-ray activity–Rossby number diagram. These relations can be further refined through improved estimates of Rossby numbers and more precise measurements of UV and chromospheric activity indices derived from high-resolution spectra. Stellar metallicity is also expected to play a significant role in the generation of stellar activity (Karoff et al. 2018); better constraints on metallicity can help reduce the scatter in these relations. Exploring such multiwavelength correlations provides valuable insights into the structure and evolution of stellar atmospheres and their underlying magnetic activity processes.

5 Stellar Flares

5.1 Solar-Type Stars

'Solar-type stars' are stars with a structure similar to our Sun, i.e. with a convective envelope and a radiative core. They encompass, roughly, the main sequence from F to M stellar types.[3] The key phenomenology that grants their definition as a class is the presence of an outer, hot atmospheric layer above their photosphere. The photosphere is optically thick and heated directly by the heat flux from the stellar interior. Pure thermodynamics arguments would imply that the temperature should decrease above the photosphere. Yet, in our Sun we clearly see—when the Sun is observed at UV, extreme-UV and X-ray wavelengths—that the temperature above the photosphere increases, first gradually to tens of thousands of K (in the chromosphere) and then sharply to hundreds of thousands of K (in the transition region), reaching millions of K in the extended outer layer, the corona.

[3]Note that the coolest M dwarfs do not have a radiative core; they are fully convective.

The driving force that creates this hot extended atmosphere is the Sun's magnetic field, generated by our star's internal dynamo, which is likely driven by the interaction between the Sun's (differential) rotation and convection in the outer layer. The Sun's magnetic field is relatively weak in the photosphere, where gas pressure dominates magnetic pressure (i.e. $\beta \gg 1$), so that the photosphere is almost entirely structured by gravity and stellar rotation (even though sunspots are a visible effect of the magnetic field's concentration).

As we ascend from the photosphere, and thus encounter hotter plasma, the gas remains optically thin, and it increasingly departs from spherical symmetry. In fact, its pressure decreases (owing to the prevailing, much lower ambient density), so that one transitions from a regime in which $\beta \gg 1$ to a regime in which $\beta \ll 1$, i.e. one in which the plasma is structured and confined by the magnetic field. The magnetically confined plasma is constantly heated by magnetic-field reconnection (through processes whose details are still not entirely clear), resulting in an outer atmospheric regime that is much hotter than the photosphere.

The Sun is thus far from being the perfect, unchanging object of Aristotelian physics, and thanks to these mechanisms it emits across a range of wavelengths much more energy than would be implied by its relatively modest photospheric temperature. These wavelengths range from the UV all the way to energetic gamma-rays, as well as non-thermal radio emission. This broad non-photospheric emission, the 'stellar activity', is powered by the combination of convection and rotation.

X-ray and extreme-UV observations from space have shown that the Sun's magnetic fields confine the plasma into thin 'loops', semicircular structures emerging from sunspots and creating 'plasma bottles' within which the plasma moves essentially uni-dimensionally, along the field lines. The first outer atmospheric layer is the chromosphere, immediately above the photosphere, which, while optically thin (unlike the photosphere) reaches about 20,000–35,000 K some 2000 km above the photosphere. Above the chromosphere lies the transition region, where the temperature rises sharply to some 1–5 MK some 100–500 km above the chromosphere. The transition region is followed by the corona, which in the Sun hosts plasma at temperatures of several MK. Both the transition region and the corona are optically thin.

Whereas the chromosphere is still gravity-structured, so that it can be envisaged as a spherical layer overlying the photosphere, the corona is highly structured, with the plasma concentrated in magnetically confined loops. And whereas coronal plasma typically emits in X-rays (given its temperature), chromospheric and transition-region plasmas emit in the UV to extreme-UV regime. These structures can be observed and studied in detail in the Sun thanks to the very high spatial resolution at a range of wavelengths and specific plasma diagnostics reached by the current generation of solar space telescopes.

Although the Sun's photospheric emission is extremely constant, with a modulation of parts in 10,000 during the solar cycle owing to the varying area covered by sunspots and faculae, the emission caused by stellar activity is highly variable, with the degree of variability increasing with decreasing wavelength (and thus increasing plasma temperature). In fact, the solar X-ray emission, which has been monitored continuously for decades by the *GOES* (Geostationary Operational Environmental Satellite) series of space-weather satellites, hardly shows a basal level of emission, and visual inspection of the light curves shows them to be the result of the superposition of a continuous series of impulsive events of varying peak luminosity and duration: for a relevant example, see Fig. 6.

These impulsive events show a typical fast, almost impulsive rise (pointing to an impulsive heating event) followed by a slower, exponential decay. They are broadly grouped under the general category of 'flares'. Detailed space-borne observations of the Sun which commenced with the Solar Maximum Mission (*SMM*) have enabled detailed studies and understanding of the flaring mechanism. It typically starts with the release of impulsive energy

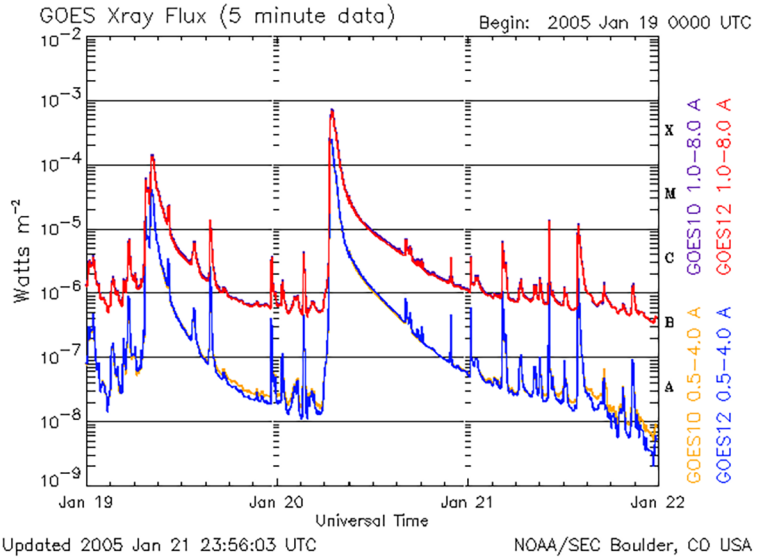


Fig. 6 Example *GOES* solar X-ray flux (5-min averaged data) recorded between 19 and 22 January 2005, showing solar soft X-ray emission in two wavelength bands: 0.5–4.0 Å (yellow and blue) and 1.0–8.0 Å (purple and red). Several major solar flares are evident as sharp flux increases, with classification levels (A, B, C, M, X: very weak, small, moderate, large and major flares, respectively) indicated on the right-hand axis. (Data from the U.S. National Oceanic and Atmospheric Administration/Space Environment Center *GOES* 10 and *GOES* 12 satellites)

close to the top of the flaring structure, resulting in a flow of particles that travels almost freely along the magnetic field lines in the corona, until it hits the denser chromosphere and photosphere. At that point, the lower layers are heated and plasma evaporates, filling the flaring loop with hot plasma, which will radiate in X-rays (while cooling) through its radiation as well as its conduction to the lower atmosphere.

Flares in the Sun are observed to have a power-law intensity distribution (e.g., Sakurai 2022), with a large number of small flares and a small number of rarer, more intense flares. Solar flares have been observed across a wide range of wavelengths, from radio waves to visible light, UV, X-rays and gamma-rays. Spatially resolved observations of solar flaring events made possible by space observatories, pioneered by *SMM* in the early 1980s, enabled the development of a 'standard model' of solar flares. In this model (see, e.g., Benz 2017, their Fig. 13), the plasma in a coronal loop is heated impulsively at the top by a magnetic reconnection event, with the energy release consisting of accelerating particles. The energetic particles then precipitate to the chromosphere, where they heat the plasma to the high temperatures observed in soft X-rays. The hot plasma then expands along the loop into the corona, a process referred to as evaporation.

When energetic electrons (and possibly ions) hit the dense underlying chromosphere via Coulomb collisions (interactions between charged particles mediated by the electrostatic force, causing energy and momentum exchange), they lose energy, the temperature in the chromosphere increases and the resulting pressure exceeds the ambient chromospheric pressure, with plasma thus flowing back into the loop. The evaporated hot plasma appears to be the source of most of the observed soft X-ray emission. This qualitative scenario explains the features observed in most (but not all) solar flares and has served remarkably well as explanatory framework for decades.

5.2 Lower-Mass Stars

Stellar activity, including flaring, is common in solar-type stars, with the relevant phenomena becoming proportionally more intense in lower-mass stars. Traditionally, a specific class of stars was defined, flare stars or UV Ceti-type variable stars, and the first instance of significant variability in the optical range was reported by Adriaan van Maanen (1884–1946) in 1945 (see the discussion in Joy 1954). This was based on photographic-plate observations of WX Ursae Majoris (WX UMa) and YZ Canis Minoris (YZ CMi), which were observed to brighten by about 1.5 mag for some tens of minutes. Once photoelectric detectors allowed continuous stellar light-curve monitoring, flaring appeared to be common in low-mass stars, with the flaring intensity increasing with decreasing wavelength, i.e. with flares manifesting more strongly in the blue and UV ranges.

In fact, modern high-cadence observations of low-mass stars show that their near-UV emission, both in the continuum and the lines (e.g., the Ca II H and K lines) is the superposition of a near-continuous series of flaring events of varying intensity, as for example shown by Kowalski et al. (2016) for YZ CMi and by Kowalski (2024a, their Fig. 1) for α Cen C. Once one moves to the UV regime, flaring is therefore no longer an exceptional event but rather the normal regime where these stars emit in the UV (as well as in higher-energy bands).

In the UV the flaring emission observed is the result of two different phenomena, with very different characteristics. On the one hand, there is the optically thin emission from the heated, optically thin chromosphere that is typically observed in the form of line emission, with a few lines dominating the UV spectrum between Lyα and the visible range. On the other hand, the photosphere, being dense and optically thick, will form a hotspot where the energy has been deposited, which will radiate the energy thermally, exhibiting a (near-) blackbody spectrum. Emission in the extreme-UV is produced largely within the transition region, with mechanisms similar to those operating in the chromosphere.

The Lyα line (at 1216 Å) is by far the strongest emission line in the solar UV spectrum, and in low-mass M dwarfs it carries by itself as much energy as the rest of the UV spectrum combined (France et al. 2012a). However, its use as a diagnostic is limited, by both astrophysical challenges (because of its strength, the assumption of optical thinness is easily challenged) and observational challenges from low-Earth orbit, where geocoronal emission from the Earth's atmosphere often contaminates the observed Lyα flux.

Stellar flares in the UV generally exhibit rapid time evolution (e.g., Brasseur et al. 2019). However, one should keep in mind that the number of stellar flares observed with good time coverage and high-quality data is limited, given that flares are stochastic events and their observation is largely a matter of luck. In fact, only a very small number of flares have been observed in the UV, and even fewer have been analysed through their rise and decay phases (for a list of the observations, see the review by Kowalski 2024a), so that the detailed behaviour of the Sun's chromospheric emission during intense flares is still not known in sufficient detail.

The behaviour of the photosphere is, by contrast, much better known thanks, first, to the numerous ground-based campaigns to observe flaring stars in the *U* band and also to the large number of stars that have been monitored in white light by *Kepler* and *TESS* while searching for exoplanetary transits. Ground-based campaigns have been carried out with relatively small telescopes, so that long observing campaigns could be dedicated to individual objects, thus significantly raising the likelihood of observing a large, well-sampled flaring event. These observations essentially monitor in a limited number of bands ranging from the atmospheric cut-off in the UV to the red part of the spectrum. This can effectively

be combined with observations of the emission in the Ca II lines and in the Balmer series (for a well-studied flare on the M dwarf YZ CMi, see, e.g., Kowalski et al. 2013), which thanks to their being ground-based can reach a coverage and data quality thus far very rare for space-borne observations.

Although the detection of stellar flares in the *TESS* and *Kepler* light curves is done in white (visible) light, these detections are relevant in the context of UV astronomy because they cover the red tail of the blackbody emission from the heated stellar photosphere. The blackbody temperature will be such that the bulk of its radiation is emitted in the UV. The temperature of the photospheric blackbody can only be inferred through broad-band colourimetry (which often includes the Balmer jump), and values ranging from $T \approx 8500$ K up to 50,000 K have been reported in the literature. At such temperatures, the bulk of the emission will be in the UV, even though this is, because of purely observational constraints, rarely observed.

Despite concentrating on the tip of the proverbial iceberg (white-light emission), *TESS* and *Kepler* observations have enabled the study of statistically large samples of stars, resulting in a number of studies of, e.g., the frequency distribution of flares as a function of their energy output, as well as the high-energy tail of the distribution, where rare, large-scale events take place. Some optical flares detected by *TESS* and *Kepler* show peak enhancements of the white-light output of the star of tens of per cent of the star's quiescent luminosity. Given that only a small fraction of the flare emission will be emitted in white light (depending on the photospheric blackbody temperature), we can only imagine how glaringly bright such events will be when observed in the UV and hope that an upcoming generation of space-borne observatories will enable UV observations of such events.

In fact, whether or not the Sun's photospheric emission can be adequately described by a blackbody spectrum remains fiercely debated. Modern high-precision irradiance measurements reveal systematic deviations caused by line blanketing and radiative-transfer effects (e.g., Thuillier et al. 2003; Gray 2005; Meftah et al. 2018). Although increasingly sophisticated models have been developed, incomplete wavelength coverage and calibration uncertainties continue to limit progress (Cessateur et al. 2016).

In conclusion, while decades of observations, both ground-based and space-borne, have advanced our knowledge and understanding of stellar flaring events quite significantly, very few large flares have been observed in detail in the UV. This is important not only because of our understanding of stellar atmospheres, but also because many phenomena such as atmospheric erosion (also caused by CMEs), photochemistry, etc. are driven by the activity of the parent stars. Understanding the dynamics, and the emission, of the most energetic events is thus necessary to understand the evolution of exoplanets, with implications for questions pertaining to habitability. We thus hope that a new generation of cost-effective space-borne UV observatories will enable the observation and understanding of stellar flares to advance significantly.

6 UV Studies of Supernovae: An Early-Time Perspective

6.1 Shock Breakout

Massive stars, with masses $> 8.5 M_{\odot}$, end their exothermic lives through gravitational core collapse. This eventually results in a SN explosion, leaving behind remnants that are both compact (e.g., a neutron star/NS, a quark star or even a stellar mass black hole/BH) and nebular (the SN remnant). The SN shock transports the gravitational binding energy of the

collapsing stellar core ($GM^2/r \sim 10^{51}$ erg) from the edge of the proto-NS to the outer layers of the progenitor. In the process, it imparts both thermal and kinetic energy to the outer layers of the erstwhile progenitor, ionising them and pushing them outwards. For matter at a local optical depth τ and a physical depth d, radiation trapping occurs as long as the diffusion timescale of the photons ($\propto \tau^2 d/c$) is shorter than the shock-propagation timescale, and radiation pressure contributes to shock propagation. As the shock plows into layers with lower optical depth, photons from the heated ejecta diffuse out faster than the local shock velocity, v. At this point, a radiative precursor exhibits a sharp surge in luminosity since thermal X-ray and UV photons break out of the shock front. This situation, which occurs when $\tau \lesssim c/v$, is known as 'shock breakout' and marks the beginning of the SN explosion (see Klein and Chevalier 1978; Blinnikov et al. 2013; Waxman and Katz 2017, and references therein). For v in the range 10^{3-4} km s^{-1}, this surge occurs at $10 \lesssim \tau \lesssim 100$, i.e. well below the stellar photosphere at $\tau = 1$. Following SBO, the stellar envelope expands and cools nearly adiabatically, resulting in shock-cooling emission.

The fireworks that result from this terminal, explosive event are thus heralded by a flash (of $\sim 10^{3-4}$ s duration) of photons whose non-Planckian spectrum (Falk 1978) peaks in the soft X-ray band, although with significant contributions in the far- and near-UV bands. In most stars with extended outer layers, the diffusion timescale ($t_{\rm diff}$) is comparable to the dynamical timescale ($t_{\rm dyn}$, defined as the time required for the break-out layer to expand to twice its thickness), and thus the diffusion region remains tied to the Lagrangian coordinate (i.e. the mass element) where the SBO occurred. The physical radius at the SBO, the duration of the flash and the peak luminosity of the burst will all depend on the total energy radiated, which is itself a function of shock strength as well as of the progenitor's density and opacity profile. In turn, they will also determine the characteristics of the resulting light curves and spectra.

Note that SBO is expected even in thermonuclear (Type-Ia) SNe, which occur via runaway thermonuclear burning in low-mass ($< 8 M_\odot$), degenerate (He or CO white-dwarf) progenitors, members of either singly or doubly degenerate binary systems. The explosion model for these events is still under debate, with both deflagration (see Fink et al. 2014, and references therein) and detonation (see Seitenzahl et al. 2013; Pollin et al. 2026, and references therein) mechanisms considered plausible. However, the detection of SBOs in Type-Ia SNe would also play an important role in reconciling the two possible mechanisms, via the delayed detonation transition model, which would begin as a subsonic deflagration and transition into a supersonic detonation (see Piro et al. 2010, and references therein). Initial simulations by Piro et al. (2010) show that the SBO in this brightest class of SNe would be extremely fast ($\sim 10^{-2}$ s), faint ($\sim 10^{40}$ erg) and peak in the hard X-ray (~ 20 keV) band. Alternatively, if the progenitor's structure allows $t_{\rm dyn} \gg t_{\rm diff}$, planar cooling could increase the overall radiated luminosity, thus making its detection possible. Such a situation could occur during SBO in Type-Ia SNe with CO progenitors, initiated via a detonation of the outer He layer, followed by a final, terminal detonation of the CO layer (Piro and Nakar 2026). This double detonation transition mechanism results in an aspherical SBO, with a relatively faint X-ray surge of $\lesssim 10^{41}$ erg lasting only $\lesssim 10$ s. However, this is followed by soft X-ray-bright (10^{43} erg), short-lived (~ 4 s) post-break-out planar cooling, unique to progenitors with He outer layers, and then 12–24 hr-long UV-dominated shock-cooling emission.

Core-collapse SNe (CC-SNe) comprise a zoo of distinct subtypes, resulting from stripped-envelope progenitors (Types Ib/Ic) as well as progenitors with extended H envelopes (Types II-P/L). Additionally, massive stars often undergo mass loss during their post-main-sequence evolution via line-driven winds or convective overshooting (when convective motions penetrate into adjacent stable layers beyond the formal convective boundary,

causing extra mixing and affecting stellar structure and surface phenomena), resulting in the formation of a circumstellar medium (CSM) whose density profile and morphology traces its evolutionary history. Narrow-line SNe result from these progenitors, cocooned within an extended, dense CSM, and they are highly diverse in their presumed pre- and known post-explosive properties (to explore CC-SNe diversity, see Hiramatsu et al. 2026, for Type-IIn); for Type-Icn and for CC-SNe in general, see Pellegrino et al. (2022) and Maeda et al. (2012), respectively. Finally, nearly ∼50 per cent of massive progenitors are expected to have had a binary companion at some point during their evolution (Zapartas et al. 2019). As can be expected, the SBO characteristics of CC-SNe are also diverse. Several studies have focussed on SBOs in these progenitors, the implications of which are briefly discussed below.

6.2 UV Modelling at the Supernova Shock

Theoretically, both analytical and numerical attempts have been made to estimate the strength and duration of UV emission at the SBO for CC-SNe. Three-dimensional (3D) simulations of SBOs in red-giant progenitors of Type-IIP SNe (Goldberg et al. 2022), the most numerous sub-class of CC-SNe, show an asymmetric breakout duration of ∼3–6 hr, spanning a range of radiative temperatures. This is in agreement with observations (e.g., Gezari et al. 2008, 2015), although the predicted luminosities are somewhat lower ($L_{\rm bol} \sim 10^{44}$ erg s^{-1}). Their 3D simulations appear to eliminate the possibility of using observed rise times to measure the stellar radius via light-travel time effects. The effect of a dense CSM on the SBO was investigated by Balberg and Loeb (2011), who used a forward–reverse shock structure for shocked ejecta interacting with the pre-existing wind to establish an analytical relation between the SBO radius and velocity, which they used to estimate the progenitor radius of the X-ray/UV-bright Type-Ibc SN2008D. Their results are in agreement with direct estimates from early X-ray and UV detections of this event (Rabinak and Waxman 2011).

More detailed numerical simulations have been carried out by De La Rosa et al. (2017), who assumed a single-temperature (for matter and radiation) photon diffusion model coupled with an homologous outflow (the LANL code) to model the UV light curves of the Type-IIn SNe (with well-studied precursor activity) SN 2009ip and SN 2011ht from SBO to the late nebular phase. They used progenitor masses in the range of 15–35 $M_\odot$ for SN2009ip and 20–45 $M_\odot$ for SN2011ht and found that while the peak of the UV light curve is determined by the shock temperate and the explosion energy, $E_{\rm expl}$, the profile depends on the mass of the ejecta as well as on $E_{\rm expl}$.

Next, a simulation of the number of events from which SBOs would be detected with a dedicated X-ray+UV wide-field survey instrument has been carried out by Bayless et al. (2022). They modelled the UV emission from CC-SNe in red-supergiant (RSG), blue-supergiant (BSG) and a range of Wolf–Rayet (WR) progenitors using the same code, assuming solar metallicity and incorporating electron scattering-dominated 'grey' opacity. They found that the duration of the UV flash at the SBO ranges from only 400 s for some RSG models to up to 10,000 s for some WR calculations (see their Table 2). Additionally, assuming a limiting UV flux of 8.0×10^{-14} erg s^{-1} cm^{-2}, they determined that over a 2 yr period, ∼ 5000 events with RSG progenitors, ∼ 3700 events with WR progenitors but only ∼ 200 events with BSG progenitors could be detected at the 3σ confidence limit (see their Table 4).

We now address the question of the actual detection of the SBO's UV component. In the absence of X-ray/UV surveys of the transient sky (although the *Einstein Probe* X-ray satellite and the proposed *ULTRASAT* mission look promising in this context), direct UV detection of SBOs has been mainly serendipitous. Although early-time UV detections of several Type-II events are available—notably, Type-IIpec SN 1987A, Type-IIb SN 1993J

and Type IIP SN 2006bp, as well as multiple events in the *Swift*/UVOT bands—these have all been detected in the shock-cooling phase. The earliest detections of actual SBO (i.e. UV brightening) were obtained for the Type-IIP SNe SNLS-04D2dc and SNLS-06D1jd, discovered by the Supernova Legacy Survey (SNLS; see Gezari et al. 2008, and references therein), followed by the *GALEX* near-UV detection of the Type-IIP SN PS1-13arp (Gezari et al. 2015). Shock–CSM interaction has been detected since then in both early and late phases. Notably, the Type-IIn SN2007pk was detected by *Swift*/UVOT ~ 5 days post-SBO (Pritchard et al. 2012). Note, however, that SBOs in interacting SNe (of which Type-IIn and Type-IIbn are subtypes) depend on the poorly understood density profile of the transition region between the progenitor and the CSM. Inkenhaag et al. (2025) searched the fields of view of 51 CC-SNe from their *HST* snapshot survey, taken within five years of discovery. They found late-time (2–4 yr) UV rebrightening only for ASAS-SN-17qp and ATLAS17lsn, which they attribute to very late-time interaction of the SN shock with the CSM.

The very early-time spectra of SNe across all classes appear to be dominated by a continuum which peaks in the UV. In many instances, also superimposed are narrow lines emitted from overlying, slowly moving material, often tenuous CSM. The narrow features may be fleeting (i.e. appearing for only a few days or, at most, a week) for all but the class of 'interacting' SNe, the best-known of which are the Type-IIn. SBO in Type-IIn SNe—whose progenitors have extended CSM—is expected to be delayed owing to their extended winds, but, assuming a density profile for the wind, can yet be used to constrain the combination of explosion energy and ejecta mass (Balberg and Loeb 2011). Whereas the flash ionisation lines themselves are indicators of the morphology and composition of the CSM, however tenuous, this is probably the only epoch in a SN's lifetime when a thermal continuum can be unequivocally identified and isolated in its spectra, thus permitting direct estimation of the velocity and temperature at the SBO. By extension, assuming reasonable values for $E_{\rm expl}$, these can be correlated with progenitor radius and mass.

In summary, at the start of the emerging era of large-scale time-domain surveys (including the Legacy Survey of Space and Time undertaken with the Vera Rubin Observatory), when rapid follow-up of transients will soon become the norm, there is an imperative need for dedicated rapid follow-up, highly sensitive, X-ray and UV transient 'factories' to make full use of this opportunity to study the final moments of the poorly understood final stages of the evolution of massive (and less massive) stars.

7 Beyond the Milky Way: Tracing Star Formation in the Magellanic Clouds Using UV Diagnostics

Our Galaxy is accompanied by many dwarf galaxies, including the Large and Small Magellanic Clouds (LMC and SMC, respectively). Located at distances of $D_{\rm LMC} \sim 50$ kpc and $D_{\rm SMC} \sim 62$ kpc (de Grijs et al. 2014; de Grijs and Bono 2015; Pietrzyński et al. 2019; Graczyk et al. 2020), their close proximity enables observation of their resolved stellar populations. Moreover, their metal-poor environments ($Z_{\rm LMC} = 0.5\,{\rm Z}_\odot$ and $Z_{\rm SMC} = 0.2\,{\rm Z}_\odot$; Dobbie et al. 2014; Choudhury et al. 2018, 2021; Hocdé et al. 2023) provide conditions analogous to those in the early Universe. Together, these properties render the Magellanic Clouds among the best laboratories for investigating how low-metallicity environments influence star formation (Kennicutt 1998; Hota et al. 2024b), massive-star evolution and the stellar feedback processes that regulate galaxy evolution.

Their young stellar populations encode the galaxies' recent evolutionary history, preserving signatures of tidal interactions, morphological transformations and the physical

mechanisms regulating star formation. The ongoing dynamical interaction of the Magellanic Clouds with each other and with the Milky Way (Harris and Zaritsky 2009; Rubele et al. 2018; Massana et al. 2022) continues to shape their current star-forming activity, thus linking the study of the Magellanic Clouds not only to local galaxy evolution but also to processes that governed star formation in the early Universe. In addition, their rich populations of young massive stars provide a direct link between recent star formation and the progenitor populations of transient sources, including CC-SNe and other endpoints of massive-star evolution, including neutron stars and black holes. Consequently, UV studies of the Magellanic Clouds also offer key insights into the environments that shape stellar activity and the production of transient events (Smartt 2009; Conroy 2013).

UV observations are particularly powerful tracers of recent star formation, since galactic emission from young, massive stars dominates the UV continuum (Kennicutt 1998; Conroy 2013). Unlike in optical or near-infrared bands, where evolved stellar populations contribute significantly, the UV is far less contaminated by older stars (Salim et al. 2007). This sensitivity allows UV diagnostics to probe young stellar populations directly, offering insights into the intensity and spatial distribution of recent star formation. Moreover, because massive stars are the primary drivers of stellar feedback through ionising radiation, stellar winds and SN explosions, UV observations provide valuable insights into the processes that shape the surrounding ISM and regulate subsequent star formation. UV observations are especially valuable in low-metallicity systems such as the Magellanic Clouds, where the reduced dust content mitigates extinction compared with more metal-rich galaxies (Gordon et al. 2003). These conditions also influence the evolution of massive stars, their feedback mechanisms and the nature of the compact remnants and transient phenomena they ultimately produce. In this section, we highlight how UV observations have advanced our understanding of the recent star-formation history, spatial structure, kinematics and hierarchical organisation of young stellar populations in the Magellanic Clouds.

Over the course of the last three decades, consecutive UV space missions, from the Ultraviolet Imaging Telescope (*UIT*; Parker et al. 1998; Cornett et al. 1997) through *GALEX*, *Swift*/UVOT and the *AstroSat*/Ultra Violet Imaging Telescope (UVIT; Tandon et al. 2017a,b), including the *HST*, have provided valuable insights into the recent star-formation activity in the Magellanic Clouds and the characteristics of their young massive stars. These surveys have enabled investigations ranging from individual massive stars and stellar clusters to galaxy-wide studies of recent star formation and stellar structure. The far-UV catalogue compiled by Parker et al. (1998) and Cornett et al. (1997) includes 37,333 sources in the LMC and 11,306 sources in the SMC. The near-UV catalogue of the LMC of Simons et al. (2014) based on *GALEX* data contains around 6 million sources. More recently, Ludwig et al. (2026) published UV catalogues for both Magellanic Clouds using UVOT, covering a total of 734,869 objects. Together, these catalogues provide an unprecedented census of UV stellar populations across the Magellanic Clouds, enabling detailed studies of their recent star-formation history, stellar clustering, spatial structure and the properties of young massive stars.

Among current UV facilities, UVIT offers a major advance for the study of the Magellanic Clouds owing to its high spatial resolution of $1''.2$–$1''.4$ and simultaneous far- and near-UV imaging capabilities. The improved resolution relative to earlier UV surveys enables the identification and characterisation of individual young stellar populations and star-forming structures across the Magellanic System. Using UVIT observations, Hota et al. (2024b) identified approximately 76,800 sources across the SMC's main body and inner Wing. In a complementary study, Hota et al. (2024a) presented a far-UV catalogue of about 14,400 stars in the Shell region, located in the northeastern outskirts of the SMC. A summary of UV catalogues of the Magellanic Clouds is presented in Table 2.

Table 2 UV catalogues of the Magellanic Clouds

Telescope	Catalogue	Comments
UIT	$N_{\rm LMC} = 37,333$, $N_{\rm SMC} = 11,306$	Far-UV filter; spatial resolution $\sim 3''$ (Parker et al. 1998; Cornett et al. 1997)
GALEX	$N_{\rm LMC} \approx 6,000,000$	Near-UV filter; spatial resolution $\sim 5''$ (Simons et al. 2014)
Swift/UVOT	$N_{\rm LMC} = 471,507$, $N_{\rm SMC} = 263,362$	Three UV filters; spatial resolution $\sim 2''$ (Ludwig et al. 2026)
AstroSat/UVIT	$N_{\rm SMC} \approx 76,800$, $N_{\rm SMC\,Shell} \approx 14,400$	Far-UV filter; spatial resolution $\sim 1''.4$ (Hota et al. 2024a,b)

7.1 Recent Star Formation History, Morphology, and Kinematics of Young Stellar Populations in the Magellanic Clouds

Early UV observations revealed that recent star formation in the Magellanic Clouds is highly structured and occurs across a hierarchy of environments, including OB associations, stellar clusters and stellar complexes. Analysing four *UIT* fields covering the SMC bar, Cornett et al. (1997) identified four concentrations of UV-bright stars arranged from northeast to southwest with nearly uniform separations of about 0.5 kpc. By comparing the large-scale far-UV and Hα morphologies, they inferred a spatial and temporal progression of star formation, unfolding over the past ~20 Myr. Similarly, Parker et al. (1998) reported that the *UIT* fields encompass 47 OB associations in the LMC and 37 in the SMC, along with 102 and 74 H II regions from the catalogue of Davies et al. (1976). The far-UV data allow easier identification of the hottest OB stars compared with optical photometry, and their ionising flux shows a clear correlation with Hα emission. They found continuous star formation up to ~500 Myr for the field stars, while the star cluster populations are characterised by a best-fitting age of around 3.4 Myr, consistent with young OB associations drawn from multiple clusters. Parker et al. (1992) obtained photometry for more than 1200 stars and spectra for 43 O and 30 early-B stars in the OB associations LH 9 and LH 10. LH 10 is younger, more reddened and has a flatter stellar initial mass function (which represents the distribution of stellar masses at the time of starbirth), containing most of the earliest O stars and several near-zero-age main-sequence stars, suggesting a higher proportion of massive stars. The calculated Lyman ionising flux of the earliest stars matches the observed H II region emission, and star formation in LH 10 may have been triggered by massive stars in LH 9. UV studies further demonstrate that recent star formation is not confined to star clusters; Almoznino et al. (2005) showed that intercluster regions in the LMC can contain young stellar populations comparable to those found within star clusters as seen in a sample of far-UV stars within a $\sim 3'$ field near the edge of the LMC bar, between the bar's centre and 30 Doradus. Together, these results established that recent star formation in the Magellanic Clouds is spatially heterogeneous and strongly influenced by stellar feedback, local environmental conditions and the Milky Way–LMC–SMC interactions.

UV observations have also provided important constraints on the recent star-formation history of the SMC. Using *Swift*/UVOT data, Hagen et al. (2017a) identified three promi-

nent peaks of recent star formation in the SMC, occurring at 6–10 Myr, 30–80 Myr and around 400 Myr ago. Their analysis also showed that most of the SMC exhibits the 2175 Å dust bump, which is stronger towards the northeast and weaker in the southwest, and that the extinction curve is generally steeper than that of the Milky Way. More recently, Ludwig et al. (2026), using UVOT UV colour–magnitude diagrams (CMDs), reported 522 candidate stripped stars in the LMC and 298 in the SMC. These systems provide valuable laboratories for studying binary evolution and represent an important population linking recent star formation to the progenitors of compact remnants and transient phenomena.

The kinematics of young stellar populations provide important clues to the dynamical evolution of the Magellanic System and the role of galaxy interactions in shaping recent star formation. Using UV observations in combination with astrometric measurements, recent studies have identified signatures of complex stellar motions across the Magellanic Clouds. Milone et al. (2023) presented photometry and astrometry for 113 star clusters in the LMC and SMC using *HST* data, providing differential-reddening maps and homogeneous CMDs. We detected extended main-sequence turn-offs in multiple clusters, including previously unreported cases, and showed that their morphology depends on cluster age. Proper-motion measurements allow separation of cluster members from field stars and reveal that young SMC stars exhibit elongated motions towards the LMC, providing new evidence of a kinematic connection between the two galaxies.

Hota et al. (2024b) used approximately 62,900 probable SMC far-UV stars to reveal important spatial and kinematic properties of the SMC's young populations. Far-UV stars are mainly distributed along the main sequence, giant and subgiant branches in CMDs, with about 2200 stars brighter than 15 mag in the far-UV (corresponding to masses $> 8 M_{\odot}$). The stellar surface-density distribution is notably clumpy, tracing key morphological features such as the broken bar, the inner Wing and a shell-like structure. Population-dependent density maps highlight distinct spatial patterns: Young 2 (main-sequence stars with ages of 50–400 Myr) closely resembles the overall density, whereas Young 1 (main-sequence stars younger than 50 Myr) and blue-loop stars are concentrated at the northeast and southwest of the bar, respectively. The densest regions of Young 3 (main-sequence stars with ages up to 1–2 Gyr) are located in the northeast and in the central part of the bar. More details of these populations can be found in Gaia Collaboration et al. (2021) and Hota et al. (2024b). The kinematic properties of all these populations suggest that all populations show two kinematically distinct subpopulations. Young 2 and Young 3 show kinematically cool, less dispersed (with a narrower width in the proper-motion distribution) and hot, highly dispersed (with a broad proper-motion distribution) subpopulations, whereas Young 1 and blue-loop stars exhibit two kinematically distinct cool populations. The kinematic analysis of this study points to a specific perturbation for stars younger than ~ 150 Myr in proper motion along the Right Ascension direction (PMRA), with no significant perturbation in the proper motion along the declination direction (PMDec). This can place useful constraints on the details of the most recent LMC–SMC interaction.

Using UVIT data, Hota et al. (2024a) studied the far-UV sources in the northeastern outskirts of the SMC, the Shell region, which is likely a tidally influenced region. They found a few far-UV sources younger than 7 Myr, with the majority of star formation having occurred between 60 and 300 Myr ago. The spatial distribution of far-UV stars is irregular and clumpy in this Shell region and traces two distinct morphological structures, an arm-like and an arc-like feature. The far-UV stellar distribution exhibits an outwards radial gradient across the SMC Shell, indicating that the inner SMC extends to a radius of roughly $\sim 2^{\circ}.2$. Beyond this boundary lies the arm-like structure, while the arc-like feature spans from the inner regions outwards into the SMC's periphery. The proper motions and velocity dispersion of

young far-UV stars, derived from their proper-motion distribution, are consistent with those of the SMC's main body, indicating no significant signs of tidal perturbation or disruption in this region. No evidence of propagating star formation is detected in the SMC's Shell region. Instead, most areas experienced two distinct episodes between 40 and 400 Myr ago: one at ~ 260 Myr, likely associated with the Magellanic Clouds' most recent interaction, and a younger ~ 60 Myr-old episode that may correspond to the SMC's pericentric passage around the Milky Way.

Taken together, these studies demonstrate that the young stellar populations in the Magellanic Clouds retain clear dynamical signatures of their recent interaction history. The spatial distributions, proper motions and age-dependent kinematic properties of UV-bright stars reveal how tidal encounters between the LMC, SMC and Milky Way have shaped recent star formation and the present-day structure of the Magellanic System. UV-selected stellar populations therefore provide a powerful means of linking recent star formation to the broader dynamical evolution of these interacting galaxies.

7.2 Hierarchical Star Formation

Stars can appear either as isolated field stars or as members of larger assemblies, such as clusters, stellar associations or extended complexes that span areas as large as the size of a galaxy. Star formation is initiated when dense regions within molecular clouds collapse under their own gravity. The ISM exhibits hierarchical structures across a wide range of spatial scales (Elmegreen 1993), with giant molecular clouds containing increasingly smaller and denser substructures in a fractal-like arrangement. This organisation is influenced by supersonic turbulence, magnetic fields and gravity (Elmegreen and Efremov 1996). Young stars, particularly those younger than 100 Myr, are distributed in patterns that reflect the ISM's hierarchical structure (Gouliermis et al. 2015). Observations and simulations both suggest that stellar groupings follow the ISM's fractal distribution (Elmegreen and Elmegreen 2001; Vázquez-Semadeni et al. 2017), a phenomenon often described as hierarchical, fractal or scale-free star formation (Larson 1995; Bate et al. 1998).

Hota et al. (2025) investigated the star formation traced by young massive stars (5–40 $M_\odot$) younger than 150 Myr using the catalogue of Hota et al. (2024b). They identified 236 young stellar structures composed of bright far-UV stars with high completeness. For each structure, parameters such as size, area, perimeter, surface density and stellar content were measured, with sizes spanning from a few to several hundred parsecs. The perimeter–area relation gives a fractal dimension of $D_p = 1.46 \pm 0.04$, whereas the 2D fractal dimensions from the number–size relation and the size distribution are $D_2 = 1.64 \pm 0.03$ and $D_2 = 1.31 \pm 0.16$, respectively, both consistent within 2σ. The number distribution between 30 and 1000 follows a slope of -0.8 ± 0.1, close to the expected theoretical value of -1 (Elmegreen and Falgarone 1996; Sun et al. 2018; Miller et al. 2022). The surface-density distribution is well described by a lognormal profile, and the results remain robust under different selection criteria. These structures display an hierarchical arrangement similar to that of the ISM, tracing the fractal nature of star formation up to 200 Myr. Figure 7 presents the slopes of the perimeter–area relation, the number–size relation, the size and number distributions for varying conditions for the far-UV massive stars (< 150 Myr). This indicates that in the SMC, both the Young 1 and blue-loop populations, which are younger than 200 Myr, exhibit hierarchical patterns.

A comparison of results obtained using different kernel widths shows that smaller kernel widths yield a larger number of detected structures and, consequently, higher fractal dimensions—although they may also include more noise. By contrast, larger kernel widths

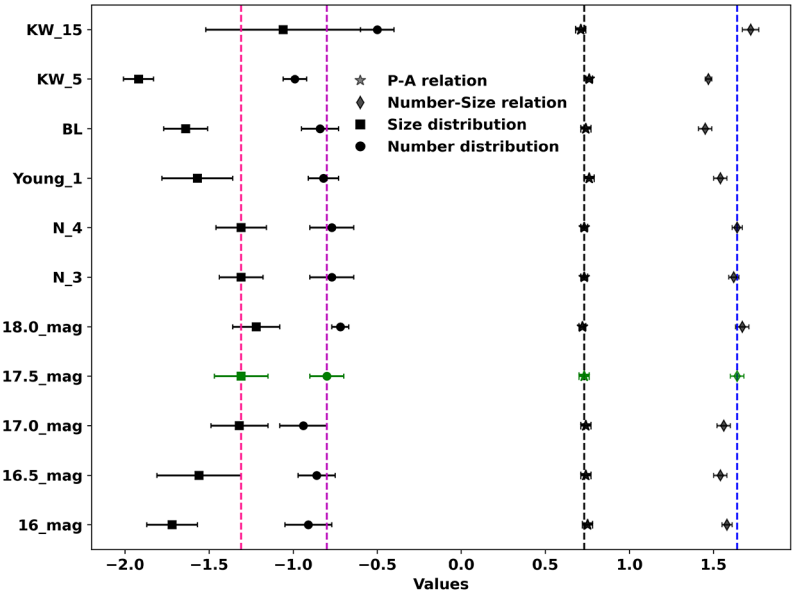


Fig. 7 Comparison of the power-law slopes obtained from the number–size, perimeter–area and size-distribution relations under different constraints, including variations in kernel width (KW), $N_{\min}$, magnitude cutoff and stellar-population composition. The dashed lines indicate the slopes derived in this study for the sample with a far-UV magnitude cutoff of 17.5 and $N_{\min} = 5$ (KW of 10 pc) (Hota et al. 2025)

produce fewer structures and lower fractal dimensions, implying a loss of genuine substructures. In addition, the fractal dimension decreases with increasing (fainter) magnitude, suggesting that the degree of hierarchy reduces with age. However, varying the minimum number cut-offs does not significantly affect the results. Table 3 presents a summary of the fractal and perimeter–area dimensions reported in different studies. It shows that the far-UV-derived massive young stellar structures exhibit dimensions comparable to those obtained for the near-infrared-identified young, low-mass stars in the SMC. This similarity suggests that the clustering behaviour of young stars is largely independent of stellar mass. It further demonstrates that these dimensions remain consistent across both local regions and the entire SMC, implying that hierarchical patterns persist on both small and large spatial scales. Moreover, despite the differences in galaxy mass of the Milky Way, LMC and SMC, the hierarchical nature of star formation seems a shared characteristic across all three systems.

7.3 Implications for Stellar Activity and Transient Phenomena

The Magellanic Clouds host a rich population of UV-bright evolved massive stars that represent key stages in the evolutionary pathways leading to transient phenomena. Their proximity and low metallicity allow individual systems to be studied in detail, providing important constraints on the physical processes governing mass loss, binary interaction and stellar feedback. UV observations are particularly sensitive to hot stellar atmospheres and circumstellar environments, making them a powerful tool for identifying and characterising populations that are often associated with transient progenitors, including WR stars, stripped stars, high-mass X-ray binaries and luminous blue variables (LBVs).

Recent UV surveys have revealed stellar populations that are directly relevant to transient studies. Using *Swift*/UVOT observations, Ludwig et al. (2026) identified 522 candidate

Table 3 Summary of estimated fractal and perimeter–area dimensions in different studies

Study	2D fractal dimension (D_2)	Perimeter–area dimension (D_P)	Comments
Hota et al. (2025)	1.31–1.64	1.46	UVIT far-UV data; massive young SMC stars
Miller et al. (2022)	1.50–1.61	1.44	VMC near-infrared data; entire LMC
Sun et al. (2018)	1.40–1.44	1.44	VMC near-infrared data; entire SMC
Sun et al. (2017a)	1.4–1.6	–	VMC near-infrared data; LMC bar
Sun et al. (2017b)	1.3–1.9	–	VMC near-infrared data; 30 Doradus (LMC)
Dickman et al. (1990), Roman-Duval et al. (2010)	–	1.3–1.6	Milky Way ISM
Stanimirovic et al. (1999, 2000)	1.4–1.5		Gas and dust, SMC
Gouliermis et al. (2014)	1.2–1.4		NGC 346 star-forming region, SMC
Tobias and Santiago (2020)	1.1–1.5		Milky Way star-forming regions

stripped stars in the LMC and 298 in the SMC. Such stars are thought to originate through binary mass transfer and represent important evolutionary channels leading to stripped-envelope SNe and compact-object binaries (Götberg et al. 2018, 2020). Their strong UV excesses make them considerably easier to identify in UV observations than in optical surveys.

UV observations have also played an important role in the study of evolved massive stars that are linked to transient progenitors. Spectroscopic investigations of WR stars and other hot massive stars in the Magellanic Clouds have provided constraints on mass-loss processes, binary interactions, and the final stages of massive-star evolution (Crowther 2003; Shkolnik and Barman 2014; Schootemeijer et al. 2024). These processes strongly influence the nature of the compact remnants and explosive events produced at the end of stellar evolution. Because radiatively driven winds depend sensitively on metallicity, the Magellanic Clouds provide an important testbed for understanding how mass-loss rates, binary evolution pathways and the production of transient progenitors differ from those observed in the Milky Way.

In addition to progenitor populations, UV observations of SN remnants have provided diagnostics of shock-heated gas and the interaction between stellar ejecta and the surrounding ISM (Raymond 1982). Such studies complement investigations of young stellar populations by tracing the long-term consequences of stellar feedback and stellar explosions.

These results demonstrate that UV observations contribute not only to our understanding of recent star formation but also to the identification of transient progenitors, the evolution of massive stars and the impact of stellar explosions on their galactic environments, particularly in the low-metallicity environments represented by the Magellanic Clouds.

8 Outlook

8.1 Photometric and Spectroscopic Perspectives for Future UV Astronomy

Throughout this review, UV diagnostics have been discussed primarily in terms of the physical information encoded in emission lines and continua. However, it is important to distinguish between the complementary roles of photometric and spectroscopic observations in extracting that information. Although both approaches probe the same underlying phenomena, they address different scientific questions and impose different requirements on future instrumentation.

UV photometry is particularly powerful for detecting variability and transient phenomena. Wide-field imaging surveys can identify stellar flares, monitor accretion variability in young stellar objects, trace star-forming regions in nearby galaxies and discover rapidly evolving transients such as SN SBOs. The principal strengths of photometric observations are their sensitivity, survey speed and temporal coverage, which enable large populations of sources to be monitored simultaneously and the discovery of rare events in real time.

Spectroscopy, by contrast, provides the physical diagnostics needed to interpret these phenomena. Measurements of line strengths, profiles and ratios yield temperatures, densities, abundances, velocity fields and mass-loss rates that cannot generally be recovered from photometry alone. Chromospheric diagnostics such as Mg II, transition-region tracers including C IV, Si IV and N V, and wind-sensitive resonance lines in massive stars all require spectroscopic observations. Similarly, understanding the energetics of stellar flares, accretion shocks, stellar winds and SN SBOs depends critically on spectroscopic measurements that reveal the physical state of the emitting plasma.

Future UV facilities will therefore benefit from maintaining a balance between these complementary capabilities. Wide-field photometric missions, such as *ULTRASAT*, will be particularly effective at identifying transient phenomena and characterising variability across stellar populations. At the same time, the eventual retirement of the *HST* highlights the need for new UV spectroscopic facilities capable of providing high-sensitivity observations over a broad wavelength range. Proposed missions such as *CETUS* (Heap et al. 2019), *UVEX* (Kulkarni et al. 2021), *CASTOR* (Côté et al. 2019, 2025) and related concepts would extend the legacy of the *HST* by enabling detailed investigations of stellar atmospheres, magnetic activity, accretion processes, stellar winds and low-metallicity stellar populations. Among these three proposed facilities, *UVEX* is unusual among survey missions because it includes spectroscopic capability, whereas *CETUS* was conceived from the outset as a spectroscopy-driven mission. *CASTOR* occupies an intermediate position with both imaging and spectroscopic modes.

Ultimately, the greatest scientific return will arise from combining these approaches. Photometric surveys reveal where and when UV variability occurs, whereas spectroscopy determines the physical mechanisms responsible for that variability. Future progress in understanding stellar activity, transient phenomena and their connection to galactic evolution will therefore depend on the continued availability of both capabilities within the UV astronomy landscape.

8.2 Outstanding Questions

UV observations remain among the most incisive yet least exploited tools for probing transient and variable astrophysical phenomena. Throughout this review, we have shown how the UV regime provides unique access to the physical processes that connect the microscopic

physics of stellar atmospheres to macroscopic phenomena such as flares, mass loss, SNe and the collective behaviour of stellar populations in galaxies. Yet despite seven decades of UV astronomy, major questions remain unanswered. Whereas the scarcity of UV data with the required cadence, sensitivity and wavelength coverage is a central limitation, theoretical uncertainties and the inherent complexity of multiscale plasma processes also continue to constrain progress.

A first set of challenges concerns stellar flares and magnetic activity. Although the Sun offers a detailed, spatially resolved example, the partition of flare energy across the spectrum remains incompletely characterised for other stars. In particular, the UV energy budget of flares is poorly constrained: how much of the released magnetic energy is radiated in chromospheric and transition-region lines such as Si IV, C IV and N V, and what fraction emerges as continuum emission from heated photospheric layers? Observations of individual events with sufficient spectral and temporal resolution are rare, and existing data sets often lack simultaneous optical and X-ray coverage. For M dwarfs and other magnetically active stars, this uncertainty directly affects models of planetary irradiation, atmospheric escape and photochemistry. A key open question is thus whether the Sun's flare-energy relationships can be generalised across spectral types and evolutionary stages, or whether low-mass stars follow fundamentally different scaling laws.

A second broad area of uncertainty lies in line formation and radiative transfer in the UV. Even for well-studied resonance transitions—Mg II h and k, C II, Si IV, C IV and He II 1640 Å—the mapping between observed profiles and the underlying thermodynamic and magnetic structures remains model-dependent. The non-LTE and scattering-dominated nature of these lines makes them exquisitely sensitive to small perturbations in temperature, density or flow velocity but difficult to invert uniquely. How can we disentangle the effects of opacity, PRD and microturbulent broadening to infer reliable physical conditions? Progress will depend on combining high-resolution spectroscopy with advanced numerical radiative transfer and magnetohydrodynamic models. Improved atomic data—particularly for collisional cross-sections and branching ratios—are equally critical.

A third outstanding challenge addresses transient events at high energies and high luminosities, notably SN SBO and the earliest phases of explosive transients. Despite the theoretical expectation that the first photons to escape a stellar envelope appear in the far-UV or soft X-rays, only a handful of direct detections exist. The scarcity of these observations reflects both the short-lived nature of SBOs—minutes to hours—and the limited sky coverage of past UV missions. The coming decade(s), with missions such as *ULTRASAT* and proposed wide-field UV imagers, may finally provide the continuous, high-cadence monitoring needed to capture these fleeting events routinely. Such data would not only constrain progenitor radii and circumstellar structures but also bridge the long-standing observational gap between late-time optical light curves and early theoretical models of explosion physics.

A fourth line of inquiry concerns stellar activity cycles and rotation–activity relations. Although large optical and X-ray surveys have revealed empirical correlations with Rossby number and rotation period, their UV counterparts remain sparse. Does the same two-regime (saturated/unsaturated) behaviour hold in the UV, and how does the UV emission evolve with stellar age and metallicity? Establishing robust relations between UV flux, rotation and convection would enable a unified dynamo framework applicable from the youngest PMS stars to the oldest solar analogues. Multiwavelength surveys that combine photometry, spectroscopy and time-domain coverage are essential to extend these correlations and test their universality.

Beyond individual stars, the extragalactic frontier of UV diagnostics poses its own set of questions. Far-UV spectroscopy of massive stars in the Magellanic Clouds has demonstrated the metallicity dependence of radiatively driven winds, yet it remains unclear whether

these relations extrapolate cleanly to the low-metallicity, high-redshift environments of early galaxies. How do massive-star winds, flare activity and feedback processes scale with metallicity, and how do they influence the integrated UV spectra used to interpret cosmic reionisation? Similarly, the hierarchical structures revealed by UV imaging of nearby star-forming regions raise fundamental questions about the universality of star-formation scaling laws and the role of feedback in shaping interstellar environments.

Finally, there is a broad, cross-cutting question concerning instrumentation and access. The field's progress has historically been constrained by the limited lifetime of UV-capable satellites and the absence of ground-based alternatives. Sustained, high-sensitivity wide-field UV monitoring—coupled with flexible follow-up capabilities—is crucial for the next generation of transient studies. Coordinated observations with optical, infrared and X-ray facilities, alongside advances in theoretical modelling and machine learning-based event classification, will be essential to unlock the full diagnostic potential of the UV regime.

In summary, the UV domain provides a uniquely sensitive diagnostic of dynamic astrophysical processes, tracing the transport of energy from stellar interiors through chromospheres, transition regions and winds, and ultimately into the surrounding ISM. By examining UV diagnostics across the spectrum of transient behaviour—from the microphysics of magnetic reconnection in stellar flares to the macroscopic shocks of SNe and the collective star-formation patterns of galaxies—in this review we have aimed to illustrate how a single, specific wavelength regime can unite the physics of stars, planets and galaxies. The synergy among solar, stellar and extragalactic UV studies is now clearer than ever: the same resonance lines that trace chromospheric heating in the solar atmosphere illuminate the earliest light from exploding stars and shape the spectra of distant galaxies. As we move into an era of rapid, wide-field transient discovery, the UV will remain indispensable—not only as a tracer of energy release and variability, but as a means of connecting the smallest and largest scales of cosmic evolution. Indeed, as we enter a new era of time-domain and multi-messenger astronomy, the UV remains the bridge between the hot, dynamic microphysics of stellar surfaces and the luminous, evolving Universe beyond.

Acknowledgements This article is part of a collection of reviews resulting from the April 2025 Workshop on 'Space-based stellar astrophysics in the UV' organised at the International Space Science Institute–Beijing. We are grateful to the institute's staff for excellent organisational and generous financial support. Richard de Grijs acknowledges financial support in the form of a Distinguished Senior Fellowship from the President's International Fellowship Initiative (PIFI), Chinese Academy of Sciences (Grant No. 2025PVA0007). Ana I. Gómez de Castro acknowledges support from the Spanish Ministry of Science, Innovation and Universities through Research Grant PID2020-116726RB-I00.

Funding Information No financial support was received beyond that disclosed in the acknowledgements.

Declarations

Competing Interests The authors declare no competing conflicts of interest of any kind.

Open Access This article is licensed under a Creative Commons Attribution 4.0 International License, which permits use, sharing, adaptation, distribution and reproduction in any medium or format, as long as you give appropriate credit to the original author(s) and the source, provide a link to the Creative Commons licence, and indicate if changes were made. The images or other third party material in this article are included in the article's Creative Commons licence, unless indicated otherwise in a credit line to the material. If material is not included in the article's Creative Commons licence and your intended use is not permitted by statutory regulation or exceeds the permitted use, you will need to obtain permission directly from the copyright holder. To view a copy of this licence, visit http://creativecommons.org/licenses/by/4.0/.

References

Abgrall H, Roueff E, Launay F, Roncin J-Y, Subtil J-L (1993a) Table of Lyman band system of molecular hydrogen. Astron Astrophys Suppl Ser 101:273–321

Abgrall H, Roueff E, Launay F, Roncin J-Y, Subtil J-L (1993b) Table of the Werner band system of molecular hydrogen. Astron Astrophys Suppl Ser 101:323–362

Akhila D, Mathew B, Nidhi S, Shridharan B, Arun R, Anilkumar H, Maheswar G, Kartha SS, Manoj P, Bhattacharyya S (2025) Analysis of forbidden neon emission lines in HAeBe stars using Spitzer IRS spectra. Mon Not R Astron Soc 540(4):3330–3349. https://doi.org/10.1093/mnras/staf914

Almoznino E, Brosch N, Shara M, Zurek D (2005) The deepest Hubble Space Telescope far-ultraviolet observations in the Large Magellanic Cloud. Mon Not R Astron Soc 357(2):645–655. https://doi.org/10.1111/j.1365-2966.2005.08690.x

Ardila DR, Herczeg GJ, Gregory SG, Ingleby L, France K, Brown A, Edwards S, Johns-Krull C, Linsky JL, Yang H, Valenti JA, Abgrall H, Alexander RD, Bergin E, Bethell T, Brown JM, Calvet N, Espaillat C, Hillenbrand LA, Hussain G, Roueff E, Schindhelm RN, Walter FM (2013) Hot gas lines in T Tauri stars. Astrophys J Suppl Ser 207(1):1. https://doi.org/10.1088/0067-0049/207/1/1

Armstrong DJ, Kirk J, Lam KWF, McCormac J, Walker SR, Brown DJA, Osborn HP, Pollacco DL, Spake J (2015) K2 variable catalogue: variable stars and eclipsing binaries in K2 campaigns 1 and 0. Astron Astrophys 579:A19. https://doi.org/10.1051/0004-6361/201525889

Astudillo-Defru N, Delfosse X, Bonfils X, Forveille T, Lovis C, Rameau J (2017) Magnetic activity in the HARPS M dwarf sample. The rotation–activity relationship for very low-mass stars through $R'_{\rm HK}$. Astron Astrophys 600:A13. https://doi.org/10.1051/0004-6361/201527078

Ayres TR, Fleming TA, Simon T, Haisch BM, Brown A, Lenz D, Wamsteker W, de Martino D, Gonzalez C, Bonnell J, Mas-Hesse JM, Rosso C, Schmitt JHMM, Truemper J, Voges W, Pye J, Dempsey RC, Linsky JL, Guinan EF, Harper GM, Jordan C, Montesinos BM, Pagano I, Rodono M (1995) The RIASS coronathon: joint X-ray and ultraviolet observations of normal F–K stars. Astrophys J Suppl Ser 96:223. https://doi.org/10.1086/192118

Bai Y, Liu J, Wicker J, Wang S, Guo J, Qin Y, He L, Wang J, Wu Y, Dong Y, Zhang Y, Hou Y, Wang Y, Cao Z (2018) The UV emission of stars in the LAMOST survey. I. Catalogs. Astrophys J Suppl Ser 235(1):16. https://doi.org/10.3847/1538-4365/aaaab9

Balberg S, Loeb A (2011) Supernova shock breakout through a wind. Mon Not R Astron Soc 414(2):1715–1720. https://doi.org/10.1111/j.1365-2966.2011.18505.x

Baliunas SL, Donahue RA, Soon WH, Horne JH, Frazer J, Woodard-Eklund L, Bradford M, Rao LM, Wilson OC, Zhang Q, Bennett W, Briggs J, Carroll SM, Duncan DK, Figueroa D, Lanning HH, Misch T, Mueller J, Noyes RW, Poppe D, Porter AC, Robinson CR, Russell J, Shelton JC, Soyumer T, Vaughan AH, Whitney JH (1995) Chromospheric variations in main-sequence stars. II. Astrophys J 438:269. https://doi.org/10.1086/175072

Barstow MA, Battisti A, Favata F, et al (2026) UV astronomical facilities for the 21st century. Space Sci Rev 222

Basri G, Laurent R, Walter FM (1985) Stellar activity in synchronized binaries. I. Dependence on rotation. Astrophys J 298:761–771. https://doi.org/10.1086/163658

Bate MR, Clarke CJ, McCaughrean MJ (1998) Interpreting the mean surface density of companions in star-forming regions. Mon Not R Astron Soc 297(4):1163–1181. https://doi.org/10.1046/j.1365-8711.1998.01565.x

Bayless AJ, Fryer C, Brown PJ, Young PA, Roming PWA, Davis M, Lechner T, Slocum S, Echon JD, Froning CS (2022) Supernova shock breakout/emergence detection predictions for a wide-field X-ray survey. Astrophys J 931(1):15. https://doi.org/10.3847/1538-4357/ac674c

Benz AO (2017) Flare observations. Living Rev Sol Phys 14(1):2. https://doi.org/10.1007/s41116-016-0004-3

Berdyugina SV (2005) Starspots: a key to the stellar dynamo. Living Rev Sol Phys 2(1):8. https://doi.org/10.12942/lrsp-2005-8

Bianchi L, Shiao B, Thilker D (2017) Revised catalog of GALEX ultraviolet sources. I. The all-sky survey: GUVcat_AIS. Astrophys J Suppl Ser 230(2):24. https://doi.org/10.3847/1538-4365/aa7053

Blinnikov S, Tolstov A, Sorokina E, Dolgov A (2013) Radiation hydrodynamics of supernova shock breakouts. High Energy Density Phys 9(1):17–21. https://doi.org/10.1016/j.hedp.2012.09.004

Blondel PFC, Talavera A, Djie HRETA (1993) Lyman-α emission in spectra of Herbig Ae stars. An indication of accretion?. Astron Astrophys 268:624–640

Boehm T, Catala C, Donati J-F, Welty A, Baudrand J, Butler CJ, Carter B, Collier-Cameron A, Czarny J, Foing B, Ghosh K, Hao J, Houdebine E, Huang L, Jiang S, Neff JE, Rees D, Semel M, Simon T, Talavera A, Zhai D, Zhao F (1996) Azimuthal structures in the wind and chromosphere of the Herbig Ae star AB Aurigae. Results from the MUSICOS 1992 campaign. Astron Astrophys Suppl Ser 120:431–450

Boggess A, Carr FA, Evans DC, Fischel D, Freeman HR, Fuechsel CF, Klinglesmith DA, Krueger VL, Longanecker GW, Moore JV (1978) The IUE spacecraft and instrumentation. Nature 275(5679):372–377. https://doi.org/10.1038/275372a0

Boro Saikia S, Marvin CJ, Jeffers SV, Reiners A, Cameron R, Marsden SC, Petit P, Warnecke J, Yadav AP (2018) Chromospheric activity catalogue of 4454 cool stars. Questioning the active branch of stellar activity cycles. Astron Astrophys 616:A108. https://doi.org/10.1051/0004-6361/201629518

Borucki WJ, Koch D, Basri G, Batalha N, Brown T, Caldwell D, Caldwell J, Christensen-Dalsgaard J, Cochran WD, DeVore E, Dunham EW, Dupree AK, Gautier TN, Geary JC, Gilliland R, Gould A, Howell SB, Jenkins JM, Kondo Y, Latham DW, Marcy GW, Meibom S, Kjeldsen H, Lissauer JJ, Monet DG, Morrison D, Sasselov D, Tarter J, Boss A, Brownlee D, Owen T, Buzasi D, Charbonneau D, Doyle L, Fortney J, Ford EB, Holman MJ, Seager S, Steffen JH, Welsh WF, Rowe J, Anderson H, Buchhave L, Ciardi D, Walkowicz L, Sherry W, Horch E, Isaacson H, Everett ME, Fischer D, Torres G, Johnson JA, Endl M, MacQueen P, Bryson ST, Dotson J, Haas M, Kolodziejczak J, Van Cleve J, Chandrasekaran H, Twicken JD, Quintana EV, Clarke BD, Allen C, Li J, Wu H, Tenenbaum P, Verner E, Bruhweiler F, Barnes J, Prsa A (2010) Kepler planet-detection mission: introduction and first results. Science 327(5968):977. https://doi.org/10.1126/science.1185402

Bouret J-C, Catala C (1998) Multi-line analysis of the spectra of Herbig Ae/Be stars. Astron Astrophys 340:163–177

Bouret J-C, Catala C (2000) NLTE calculations of neutral helium lines in the wind of the Herbig Ae star AB Aurigae. Astron Astrophys 359:1011–1024

Bouret J-C, Catala C, Simon T (1997) Nitrogen V in the wind of the pre-main sequence Herbig Ae star AB Aurigae. Astron Astrophys 328:606–616

Brandenburg A, Saar SH, Turpin CR (1998) Time evolution of the magnetic activity cycle period. Astrophys J Lett 498(1):L51–L54. https://doi.org/10.1086/311297

Brasseur CE, Osten RA, Fleming SW (2019) Short-duration stellar flares in GALEX data. Astrophys J 883(1):88. https://doi.org/10.3847/1538-4357/ab3df8

Brasseur CE, Osten RA, Tristan II, Kowalski AF (2023) Constraints on stellar flare energy ratios in the NUV and optical from a multiwavelength study of GALEX and Kepler flare stars. Astrophys J 944(1):5. https://doi.org/10.3847/1538-4357/acab59

Brown A, de M. Ferraz MC, Jordan C (1984) The chromosphere and corona of T Tauri. Mon Not R Astron Soc 207:831–859. https://doi.org/10.1093/mnras/207.4.831

Brun AS, García RA, Houdek G, Nandy D, Pinsonneault M (2015) The solar–stellar connection. Space Sci Rev 196(1-4):303–356. https://doi.org/10.1007/s11214-014-0117-8

Butler CJ, Byrne PB, Andrews AD, Doyle JG (1981) Ultraviolet spectra of dwarf solar neighbourhood stars. I. Mon Not R Astron Soc 197:815–827. https://doi.org/10.1093/mnras/197.3.815

Butler CJ, Rodono M, Foing BH (1988) A correlation between Balmer and soft X-ray emission from stellar and solar flares. Astron Astrophys 206:L1–L4

Calvet N, Gullbring E (1998) The structure and emission of the accretion shock in T Tauri stars. Astrophys J 509(2):802–818. https://doi.org/10.1086/306527

Carpenter KG, Robinson RD, Judge PG (1995) GHRS observations of cool, low-gravity stars. II. Flow and turbulent velocities in the outer atmosphere of γ Crucis (M3.4 III). Astrophys J 444:424. https://doi.org/10.1086/175617

Castor JI, Abbott DC, Klein RI (1975) Radiation-driven winds in of stars. Astrophys J 195:157–174. https://doi.org/10.1086/153315

Catala C (1998) Multi-site continuous spectroscopy: previous MUSICOS campaigns. In: Kaper L, Fullerton AW (eds) Cyclical variability in stellar winds, p 349

Catala C (2003) δ Scuti pulsations in pre-main sequence stars. Astrophys Space Sci 284(1):53–60. https://doi.org/10.1023/A:1023224326127

Catala C, Kunasz PB (1987) Line formation in the winds of Herbig Ae/Be stars. The Hα line. Astron Astrophys 174:158–172

Catala C, Donati JF, Böhm T, Landstreet J, Henrichs HF, Unruh Y, Hao J, Collier Cameron A, Johns-Krull CM, Kaper L, Simon T, Foing BH, Cao H, Ehrenfreund P, Hatzes AP, Huang L, de Jong JA, Kennelly EJ, ten Kulve E, Mulliss CL, Neff JE, Oliveira JM, Schrijvers C, Stempels HC, Telting JH, Walton N, Yang D (1999) Short-term spectroscopic variability in the pre-main sequence Herbig Ae star AB Aurigae during the MUSICOS 96 campaign. Astron Astrophys 345:884–904

Cauley PW, Johns-Krull CM (2016) Investigating the origin of hot gas lines in Herbig Ae/Be stars. Astrophys J 825(2):147. https://doi.org/10.3847/0004-637X/825/2/147

Cessateur G, Schmutz W, Wehrli C, Gröbner J, Haberreiter M, Kretzschmar M, Rozanov E, Schöll M, Shapiro A, Thuillier G, Egorova T, Finsterle W, Fox N, Hochedez J-F, Koller S, Meftah M, Meindl P, Nyeki S, Pfiffner D, Roth H, Rouzé M, Spescha M, Tagirov R, Werner L, Wyss J-U (2016) Solar irradiance observations with PREMOS filter radiometers on the Picard mission: in-flight performance and data release. Astron Astrophys 588:A126. https://doi.org/10.1051/0004-6361/201527577

Chahal D, de Grijs R, Kamath D, Chen X (2022) Statistics of BY Draconis chromospheric variable stars. Mon Not R Astron Soc 514(4):4932–4943. https://doi.org/10.1093/mnras/stac1660
Chahal D, Kamath D, de Grijs R, Ventura P, Chen X (2023) Unravelling the period gap using LAMOST chromospheric activity indices. Mon Not R Astron Soc 525(3):4026–4041. https://doi.org/10.1093/mnras/stad2521
Chahal D, Kamath D, de Grijs R, Montet BT, Chen X (2025) Photometric activity cycles in fast-rotating stars: revisiting the reality of stellar activity cycle branches. Mon Not R Astron Soc 540(1):668–687. https://doi.org/10.1093/mnras/staf754
Charbonneau P (2020) Dynamo models of the solar cycle. Living Rev Sol Phys 17(1):4. https://doi.org/10.1007/s41116-020-00025-6
Chen X, Wang S, Deng L, de Grijs R, Yang M, Tian H (2020) The Zwicky Transient Facility catalog of periodic variable stars. Astrophys J Suppl Ser 249(1):18. https://doi.org/10.3847/1538-4365/ab9cae
Chen Y, Peter H, Przybylski D, Tian H, Zhang J (2022) Doppler shifts of spectral lines formed in the solar transition region and corona. Astron Astrophys 661:A94. https://doi.org/10.1051/0004-6361/202243111
Chisholm J, Rigby JR, Bayliss M, Berg DA, Dahle H, Gladders M, Sharon K (2019) Constraining the metallicities, ages, star formation histories, and ionizing continua of extragalactic massive star populations. Astrophys J 882(2):182. https://doi.org/10.3847/1538-4357/ab3104
Choudhury S, Subramaniam A, Cole AA, Sohn YJ (2018) Photometric metallicity map of the Small Magellanic Cloud. Mon Not R Astron Soc 475(4):4279–4297. https://doi.org/10.1093/mnras/sty087
Choudhury S, de Grijs R, Bekki K, Cioni M-RL, Ivanov VD, van Loon JT, Miller AE, Niederhofer F, Oliveira JM, Ripepi V, Sun N-C, Subramanian S (2021) The VMC survey - XLIV: mapping metallicity trends in the Large Magellanic Cloud using near-infrared passbands. Mon Not R Astron Soc 507(4):4752–4763. https://doi.org/10.1093/mnras/stab2446
Code AD, Meade MR (1979) Ultraviolet photometry from Orbiting Astronomical Observatory. XXXII. An atlas of ultraviolet stellar spectra. Astrophys J Suppl Ser 39:195–289. https://doi.org/10.1086/190571
Code AD, Houck TE, McNall JF, Bless RC, Lillie CF (1970) Ultraviolet photometry from the Orbiting Astronomical Observatory. I. Instrumentation and operation. Astrophys J 161:377. https://doi.org/10.1086/150545
Conroy C (2013) Modeling the panchromatic spectral energy distributions of galaxies. Annu Rev Astron Astrophys 51(1):393–455. https://doi.org/10.1146/annurev-astro-082812-141017
Cornett RH, Greason MR, Hill JK, Parker JW, Waller WH, Bohlin RC, Cheng KP, Neff SG, O'Connell RW, Roberts MS, Smith AM, Stecher TP (1997) UIT: ultraviolet observations of the Small Magellanic Cloud. Astron J 113:1011–1021. https://doi.org/10.1086/118317
Côté P, Abraham B, Balogh M, et al (2019) CASTOR: a flagship Canadian space telescope. In: Canadian long range plan for astronomy and astrophysics white papers, vol 2020, p 18. https://doi.org/10.5281/zenodo.3758463
Côté P, Woods TE, Hutchings JB, et al (2025) The CASTOR mission. J Astron Telesc Instrum Syst 11:042202. https://doi.org/10.1117/1.JATIS.11.4.042202
Cranmer SR, Saar SH (2011) Testing a predictive theoretical model for the mass loss rates of cool stars. Astrophys J 741(1):54. https://doi.org/10.1088/0004-637X/741/1/54
Crowther PA (2003) Stellar parameters of Wolf-Rayet stars from far-UV to mid-IR observations. In: van der Hucht K, Herrero A, Esteban C (eds) A massive star odyssey: from main sequence to supernova. IAU symposium, vol 212, p 47. https://doi.org/10.48550/arXiv.astro-ph/0207574
Davies RD, Elliott KH, Meaburn J (1976) The nebular complexes of the Large and Small Magellanic Clouds. Mem R Astron Soc 81:89
de Grijs R, Bono G (2015) Clustering of Local Group distances: publication bias or correlated measurements? III. The Small Magellanic Cloud. Astron J 149(6):179. https://doi.org/10.1088/0004-6256/149/6/179
de Grijs R, Kamath D (2021) Stellar chromospheric variability. Universe 7(11):440. https://doi.org/10.3390/universe7110440
de Grijs R, Wicker JE, Bono G (2014) Clustering of Local Group distances: publication bias or correlated measurements? I. The Large Magellanic Cloud. Astron J 147(5):122. https://doi.org/10.1088/0004-6256/147/5/122
De La Rosa J, Roming P, Fryer C (2017) Rapidly interpreting UV–optical light curve properties using a "simple" modeling approach. Astrophys J 850(2):133. https://doi.org/10.3847/1538-4357/aa93ee
Del Zanna G, Mason HE (2018) Solar UV and X-ray spectral diagnostics. Living Rev Sol Phys 15(1):5. https://doi.org/10.1007/s41116-018-0015-3
Del Zanna G, Dere KP, Young PR, Landi E (2021) CHIANTI—an atomic database for emission lines. XVI. Version 10, further extensions. Astrophys J 909(1):38. https://doi.org/10.3847/1538-4357/abd8ce
Deleuil M, Bouret J-C, Catala C, Lecavelier des Etangs A, Vidal-Madjar A, Roberge A, Feldman PD, Martin C, Ferlet R (2005) New insights in the FUV into the activity of the Herbig Ae star HD 163296. Astron Astrophys 429:247–255. https://doi.org/10.1051/0004-6361:20041446

Dere KP, Del Zanna G, Young PR, Landi E, Sutherland RS (2019) CHIANTI—an atomic database for emission lines. XV. Version 9, improvements for the X-ray satellite lines. Astrophys J Suppl Ser 241(2):22. https://doi.org/10.3847/1538-4365/ab05cf

Devine D, Grady CA, Kimble RA, Woodgate B, Bruhweiler FC, Boggess A, Linsky JL, Clampin M (2000) A Lyα bright jet from a Herbig Ae star. Astrophys J Lett 542(2):L115–L118. https://doi.org/10.1086/312939

Diamond-Lowe H, Youngblood A, Charbonneau D, King G, Teal DJ, Bastelberger S, Corrales L, Kempton EMR (2021) The high-energy spectrum of the nearby planet-hosting inactive mid-M dwarf LHS 3844. Astron J 162(1):10. https://doi.org/10.3847/1538-3881/abfa1c

Dickman RL, Horvath MA, Margulis M (1990) A search for scale-dependent morphology in five molecular cloud complexes. Astrophys J 365:586. https://doi.org/10.1086/169512

Dikpati M, Gilman PA (2006) Simulating and predicting solar cycles using a flux-transport dynamo. Astrophys J 649(1):498–514. https://doi.org/10.1086/506314

Distefano E, Lanzafame AC, Brugaletta E, Holl B, Lanza AF, Messina S, Pagano I, Audard M, Jevardat de Fombelle G, Lecoeur-Taibi I, Mowlavi N, Nienartowicz K, Rimoldini L, Evans DW, Riello M, García-Lario P, Gavras P, Eyer L (2023) Gaia data release 3. Rotational modulation and patterns of colour variation in solar-like variables. Astron Astrophys 674:A20. https://doi.org/10.1051/0004-6361/202244178

Dobbie PD, Cole AA, Subramaniam A, Keller S (2014) Red giants in the Small Magellanic Cloud - II. Metallicity gradient and age–metallicity relation. Mon Not R Astron Soc 442(2):1680–1692. https://doi.org/10.1093/mnras/stu926

Donati J-F, Semel M, Carter BD, Rees DE, Collier Cameron A (1997) Spectropolarimetric observations of active stars. Mon Not R Astron Soc 291(4):658–682. https://doi.org/10.1093/mnras/291.4.658

D'Orazi V, Biazzo K, Randich S (2011) Chemical composition of the Taurus–Auriga association. Astron Astrophys 526:A103. https://doi.org/10.1051/0004-6361/201015616

Duvvuri GM, Pineda JS, Berta-Thompson ZK, France K, Youngblood A (2023) FUMES. III. Ultraviolet and optical variability of M-dwarf chromospheres. Astron J 165(1):12. https://doi.org/10.3847/1538-3881/ac9b49

Duvvuri GM, Pineda JS, García Soto A, Berta-Thompson ZK, Youngblood A, France K, Newton ER, Stassun KG (2025) FUMES. IV. Optical and far-ultraviolet spectra of a flare on the M dwarf GJ 4334. Astron J 170(4):249. https://doi.org/10.3847/1538-3881/adff74

Elmegreen BG (1993) Star formation at compressed interfaces in turbulent self-gravitating clouds. Astrophys J Lett 419:L29. https://doi.org/10.1086/187129

Elmegreen BG, Efremov YN (1996) An extension of hierarchical star formation to galactic scales. Astrophys J 466:802. https://doi.org/10.1086/177554

Elmegreen BG, Elmegreen DM (2001) Fractal structure in galactic star fields. Astron J 121(3):1507–1511. https://doi.org/10.1086/319416

Elmegreen BG, Falgarone E (1996) A fractal origin for the mass spectrum of interstellar clouds. Astrophys J 471:816. https://doi.org/10.1086/178009

Falk SW (1978) Shock steepening and prompt thermal emission in supernovae. Astrophys J Lett 225:L133–L136. https://doi.org/10.1086/182810

Feinstein AD, France K, Youngblood A, Duvvuri GM, Teal DJ, Cauley PW, Seligman DZ, Gaidos E, Kempton EMR, Bean JL, Diamond-Lowe H, Newton E, Ginzburg S, Plavchan P, Gao P, Schlichting H (2022) AU Microscopii in the far-UV: observations in quiescence, during flares, and implications for AU Mic b and c. Astron J 164(3):110. https://doi.org/10.3847/1538-3881/ac8107

Fetherolf T, Pepper J, Simpson E, Kane SR, Močnik T, English JE, Antoci V, Huber D, Jenkins JM, Stassun K, Twicken JD, Vanderspek R, Winn JN (2023) Variability catalog of stars observed during the TESS prime mission. Astrophys J Suppl Ser 268(1):4. https://doi.org/10.3847/1538-4365/acdee5

Fink M, Kromer M, Seitenzahl IR, Ciaraldi-Schoolmann F, Röpke FK, Sim SA, Pakmor R, Ruiter AJ, Hillebrandt W (2014) Three-dimensional pure deflagration models with nucleosynthesis and synthetic observables for type Ia supernovae. Mon Not R Astron Soc 438(2):1762–1783. https://doi.org/10.1093/mnras/stt2315

Fontenla JM, Curdt W, Haberreiter M, Harder J, Tian H (2009) Semi-empirical models of the solar atmosphere. III. Set of non-LTE models for far-ultraviolet/extreme-ultraviolet irradiance computation. Astrophys J 707(1):482–502. https://doi.org/10.1088/0004-637X/707/1/482

France K, Linsky JL, Tian F, Froning CS, Roberge A (2012a) Time-resolved ultraviolet spectroscopy of the M-dwarf GJ 876 exoplanetary system. Astrophys J Lett 750(2):L32. https://doi.org/10.1088/2041-8205/750/2/L32

France K, Schindhelm R, Herczeg GJ, Brown A, Abgrall H, Alexander RD, Bergin EA, Brown JM, Linsky JL, Roueff E, Yang H (2012b) A Hubble Space Telescope survey of H_2 emission in the circumstellar environments of young stars. Astrophys J 756(2):171. https://doi.org/10.1088/0004-637X/756/2/171

France K, Froning CS, Linsky JL, Roberge A, Stocke JT, Tian F, Bushinsky R, Désert J-M, Mauas P, Vieytes M, Walkowicz LM (2013) The ultraviolet radiation environment around M dwarf exoplanet host stars. Astrophys J 763(2):149. https://doi.org/10.1088/0004-637X/763/2/149

France K, Loyd ROP, Youngblood A, Brown A, Schneider PC, Hawley SL, Froning CS, Linsky JL, Roberge A, Buccino AP, Davenport JRA, Fontenla JM, Kaltenegger L, Kowalski AF, Mauas PJD, Miguel Y, Redfield S, Rugheimer S, Tian F, Vieytes MC, Walkowicz LM, Weisenburger KL (2016) The MUSCLES treasury survey. I. Motivation and overview. Astrophys J 820(2):89. https://doi.org/10.3847/0004-637X/820/2/89

France K, Arulanantham N, Fossati L, Lanza AF, Loyd ROP, Redfield S, Schneider PC (2018) Far-ultraviolet activity levels of F, G, K, and M dwarf exoplanet host stars. Astrophys J Suppl Ser 239(1):16. https://doi.org/10.3847/1538-4365/aae1a3

Fuhrmeister B, Liefke C, Schmitt JHMM, Reiners A (2008) Multiwavelength observations of a giant flare on CN Leonis. I. The chromosphere as seen in the optical spectra. Astron Astrophys 487(1):293–306. https://doi.org/10.1051/0004-6361:200809379

Gahm GF, Fredga K, Liseau R, Dravins D (1979) The far-UV spectrum of the T Tauri star RU Lupi. Astron Astrophys 73:L4–L6

Gaia Collaboration, Luri X, et al (2021) Gaia early data release 3. Structure and properties of the Magellanic clouds. Astron Astrophys 649:A7. https://doi.org/10.1051/0004-6361/202039588

Gershberg RE (1972) Some results of the cooperative photometric observations of the UV Cet-type flare stars in the years 1967–71. Astrophys Space Sci 19(1):75–92. https://doi.org/10.1007/BF00643168

Gezari S, Dessart L, Basa S, Martin DC, Neill JD, Woosley SE, Hillier DJ, Bazin G, Forster K, Friedman PG, Le Du J, Mazure A, Morrissey P, Neff SG, Schiminovich D, Wyder TK (2008) Probing shock breakout with serendipitous GALEX detections of two SNLS type II-P supernovae. Astrophys J Lett 683(2):L131. https://doi.org/10.1086/591647

Gezari S, Jones DO, Sanders NE, Soderberg AM, Hung T, Heinis S, Smartt SJ, Rest A, Scolnic D, Chornock R, Berger E, Foley RJ, Huber ME, Price P, Stubbs CW, Riess AG, Kirshner RP, Smith K, Wood-Vasey WM, Schiminovich D, Martin DC, Burgett WS, Chambers KC, Flewelling H, Kaiser N, Tonry JL, Wainscoat R (2015) GALEX detection of shock breakout in type IIP supernova PS1-13arp: implications for the progenitor star wind. Astrophys J 804(1):28. https://doi.org/10.1088/0004-637X/804/1/28

Giampapa MS, Worden SP, Schneeberger TJ, Cram LE (1981) Stellar model chromospheres. XII. High-resolution, absolute flux profiles of the CaII H and K lines in dMe and non-dMe stars. Astrophys J 246:502–514. https://doi.org/10.1086/158950

Goldberg JA, Jiang Y-F, Bildsten L (2022) Shock breakout in three-dimensional red supergiant envelopes. Astrophys J 933(2):164. https://doi.org/10.3847/1538-4357/ac75e3

Gómez de Castro AI (2013) Evidence of hot high velocity photoionized plasma falling on actively accreting T Tauri stars. Astrophys J 775(2):131. https://doi.org/10.1088/0004-637X/775/2/131

Gómez de Castro AI, Lamzin SA (1999) Accretion shocks in T Tauri stars: diagnosis via semiforbidden ultraviolet line ratios. Mon Not R Astron Soc 304(4):L41–L45. https://doi.org/10.1046/j.1365-8711.1999.02545.x

Gómez de Castro AI, Marcos-Arenal P (2012) Extended magnetospheres in pre-main-sequence evolution: from T Tauri stars to the brown dwarf limit. Astrophys J 749(2):190. https://doi.org/10.1088/0004-637X/749/2/190

Gómez de Castro AI, Verdugo E (2001) New constraints on protostellar jet collimation from high-density gas UV tracers. Astrophys J 548(2):976–989. https://doi.org/10.1086/318993

Gómez de Castro AI, Verdugo E (2003) Hubble Space Telescope STIS spectrum of RW Aurigae A: evidence for an ionized beltlike structure and mass ejection in timescales of a few hours. Astrophys J 597(1):443–454. https://doi.org/10.1086/378381

Gómez de Castro AI, Franqueira M, Wamsteker W (1997) International ultraviolet explorer–uniform low dispersion archive: T Tauri stars, vol 8. European Space Agency, Noordwijk

Gómez de Castro AI, Vallejo JC, Canet A, Loyd P, France K (2020) Accretion and intercycle variations in the PMS interacting binary AK Sco. Astrophys J 904(2):120. https://doi.org/10.3847/1538-4357/abbeef

Gómez de Castro AI, France K, Canet A (2026) Lessons learnt on the formation and evolution of young planetary systems from ultraviolet spectroscopy. Space Sci Rev 222:52. https://doi.org/10.1007/s11214-026-01304-8

Gordon KD, Clayton GC, Misselt KA, Landolt AU, Wolff MJ (2003) A quantitative comparison of the Small Magellanic Cloud, Large Magellanic Cloud, and Milky Way ultraviolet to near-infrared extinction curves. Astrophys J 594(1):279–293. https://doi.org/10.1086/376774

Götberg Y, de Mink SE, Groh JH, Kupfer T, Crowther PA, Zapartas E, Renzo M (2018) Spectral models for binary products: unifying subdwarfs and Wolf-Rayet stars as a sequence of stripped-envelope stars. Astron Astrophys 615:A78. https://doi.org/10.1051/0004-6361/201732274

Götberg Y, Korol V, Lamberts A, Kupfer T, Breivik K, Ludwig B, Drout MR (2020) Stars stripped in binaries: the living gravitational-wave sources. Astrophys J 904(1):56. https://doi.org/10.3847/1538-4357/abbda5

Gouliermis DA, Hony S, Klessen RS (2014) The complex distribution of recently formed stars. Bimodal stellar clustering in the star-forming region NGC 346. Mon Not R Astron Soc 439(4):3775–3789. https://doi.org/10.1093/mnras/stu228

Gouliermis DA, Thilker D, Elmegreen BG, Elmegreen DM, Calzetti D, Lee JC, Adamo A, Aloisi A, Cignoni M, Cook DO, Dale DA, Gallagher JS, Grasha K, Grebel EK, Davó AH, Hunter DA, Johnson KE, Kim H, Nair P, Nota A, Pellerin A, Ryon J, Sabbi E, Sacchi E, Smith LJ, Tosi M, Ubeda L, Whitmore B (2015) Hierarchical star formation across the ring galaxy NGC 6503. Mon Not R Astron Soc 452(4):3508–3528. https://doi.org/10.1093/mnras/stv1325

Graczyk D, Pietrzyński G, Thompson IB, Gieren W, Zgirski B, Villanova S, Górski M, Wielgórski P, Karczmarek P, Narloch W, Pilecki B, Taormina M, Smolec R, Suchomska K, Gallenne A, Nardetto N, Storm J, Kudritzki R-P, Kałuszyński M, Pych W (2020) A distance determination to the Small Magellanic Cloud with an accuracy of better than two percent based on late-type eclipsing binary stars. Astrophys J 904(1):13. https://doi.org/10.3847/1538-4357/abbb2b

Grady CA, Woodgate B, Torres CAO, Henning T, Apai D, Rodmann J, Wang H, Stecklum B, Linz H, Williger GM, Brown A, Wilkinson E, Harper GM, Herczeg GJ, Danks A, Vieira GL, Malumuth E, Collins NR, Hill RS (2004) The environment of the optically brightest Herbig Ae star, HD 104237. Astrophys J 608(2):809–830. https://doi.org/10.1086/420763

Gray DF (2005) The observation and analysis of stellar photospheres. Cambridge University Press. https://doi.org/10.1017/CBO9781316036570

Gullbring E, Hartmann L, Briceño C, Calvet N (1998) Disk accretion rates for T Tauri stars. Astrophys J 492(1):323–341. https://doi.org/10.1086/305032

Hagen LMZ, Siegel MH, Hoversten EA, Gronwall C, Immler S, Hagen A (2017a) Swift Ultraviolet Survey of the Magellanic Clouds (SUMaC) - I. Shape of the ultraviolet dust extinction law and recent star formation history of the Small Magellanic Cloud. Mon Not R Astron Soc 466(4):4540–4557. https://doi.org/10.1093/mnras/stw2954

Hagen LMZ, Siegel MH, Hoversten EA, Gronwall C, Immler S, Hagen A (2017b) Swift Ultraviolet Survey of the Magellanic Clouds (SUMaC) - I. Shape of the ultraviolet dust extinction law and recent star formation history of the Small Magellanic Cloud. Mon Not R Astron Soc 466(4):4540–4557. https://doi.org/10.1093/mnras/stw2954

Haisch BM, Harnden FR Jr, Seward FD, Vaiana GS, Linsky JL, Rosner R (1980) Einstein X-ray observations of Proxima Centauri and the surrounding region. Astrophys J Lett 242:L99–L103. https://doi.org/10.1086/183411

Harman CE, Schwieterman EW, Schottelkotte JC, Kasting JF (2015) Abiotic O_2 levels on planets around F, G, K, and M stars: possible false positives for life?. Astrophys J 812(2):137. https://doi.org/10.1088/0004-637X/812/2/137

Harris J, Zaritsky D (2009) The star formation history of the Large Magellanic Cloud. Astron J 138(5):1243–1260. https://doi.org/10.1088/0004-6256/138/5/1243

Hartmann L, Davis R, Dupree AK, Raymond J, Schmidtke PC, Wing RF (1979) Chromospheres of the active dwarf binaries EQ Pegasi and ξ Bootis. Astrophys J Lett 233:L69–L72. https://doi.org/10.1086/183078

Hartmann L, Herczeg G, Calvet N (2016) Accretion onto pre-main-sequence stars. Annu Rev Astron Astrophys 54:135–180. https://doi.org/10.1146/annurev-astro-081915-023347

Hawley SL, Pettersen BR (1991) The great flare of 1985 April 12 on AD Leonis. Astrophys J 378:725. https://doi.org/10.1086/170474

Heap S, Arenberg J, Hull T, Kendrick S, Woodruff R (2019) The NASA Probe space mission concept, Cosmic Evolution Through UV Surveys (CETUS). arXiv e-prints. arXiv:1909.10437. https://doi.org/10.48550/arXiv.1909.10437

Herczeg GJ, Linsky JL, Valenti JA, Johns-Krull CM, Wood BE (2002) The far-ultraviolet spectrum of TW Hydrae. I. Observations of H_2 fluorescence. Astrophys J 572(1):310–325. https://doi.org/10.1086/339731

Herczeg GJ, Wood BE, Linsky JL, Valenti JA, Johns-Krull CM (2004) The far-ultraviolet spectra of TW Hydrae. II. Models of H_2 fluorescence in a disk. Astrophys J 607(1):369–383. https://doi.org/10.1086/383340

Hillier DJ, Miller DL (1998) The treatment of non-LTE line blanketing in spherically expanding outflows. Astrophys J 496(1):407–427. https://doi.org/10.1086/305350

Hiramatsu D, Berger E, Gomez S, Blanchard PK, Kumar H, Athukoralalage W (2026) Type IIn supernovae. I. Uniform light curve characterization and a bimodality in the radiated energy distribution. Astrophys J 1005:82. https://doi.org/10.3847/1538-4357/ae743c. arXiv:2411.07287

Hocdé V, Smolec R, Moskalik P, Ziółkowska O, Singh Rathour R (2023) Metallicity estimations of MW, SMC, and LMC classical Cepheids from the shape of the V- and I-band light curves. Astron Astrophys 671:A157. https://doi.org/10.1051/0004-6361/202245038

Hota S, Subramaniam A, Dhanush SR, Cioni M-RL, Subramanian S (2024a) UVIT Study of the MAgellanic Clouds (U-SMAC) - I. Recent star formation history and kinematics of the Shell region in the north-eastern Small Magellanic Cloud. Mon Not R Astron Soc 532(1):322–335. https://doi.org/10.1093/mnras/stae1438

Hota S, Subramaniam A, Nayak PK, Subramanian S (2024b) UVIT Study of the MAgellanic Clouds (U-SMAC). II. A far-UV catalog of the Small Magellanic Cloud: morphology and kinematics of young stellar population. Astron J 168(6):255. https://doi.org/10.3847/1538-3881/ad7de2

Hota S, de Grijs R, Subramaniam A (2025) UVIT Study of the Magellanic Clouds (U-SMAC). III. Hierarchical star formation in the Small Magellanic Cloud regulated by turbulence. Astrophys J 989(2):216. https://doi.org/10.3847/1538-4357/adec84

Houdebine ER, Mullan DJ, Bercu B, Paletou F, Gebran M (2017) The rotation–activity correlations in K and M dwarfs. II. New constraints on the dynamo mechanisms in late-K and M dwarfs before and at the transition to complete convection. Astrophys J 837(1):96. https://doi.org/10.3847/1538-4357/aa5cad

Imhoff CL, Giampapa MS (1980) The ultraviolet spectrum of the T Tau star RW Aur. Astrophys J Lett 239:L115–L119. https://doi.org/10.1086/183305

Ingleby L, Calvet N, Herczeg G, Blaty A, Walter F, Ardila D, Alexander R, Edwards S, Espaillat C, Gregory SG, Hillenbrand L, Brown A (2013) Accretion rates for T Tauri stars using nearly simultaneous ultraviolet and optical spectra. Astrophys J 767(2):112. https://doi.org/10.1088/0004-637X/767/2/112

Inkenhaag A, Jonker PG, Levan AJ, Fraser M, Lyman JD, Galbany L, Kuncarayakti H (2025) Study of late-time ultraviolet emission in core collapse supernovae and its implications for the peculiar transient AT2018cow. Astron Astrophys 693:A39. https://doi.org/10.1051/0004-6361/202449525

Irving ZA, Saar SH, Wargelin BJ, do Nascimento J-D (2023) Stellar cycles in fully convective stars and a new interpretation of dynamo evolution. Astrophys J 949(2):51. https://doi.org/10.3847/1538-4357/acc468

Isaacson H, Howard AW, Fulton B, Petigura EA, Weiss LM, Kane SR, Carter B, Beard C, Giacalone S, Van Zandt J, Akana Murphy JM, Dai F, Chontos A, Polanski AS, Rice M, Lubin J, Brinkman C, Rubenzahl RA, Blunt S, Yee SW, MacDougall MG, Dalba PA, Tyler D, Behmard A, Angelo I, Pidhorodetska D, Mayo AW, Holcomb R, Turtelboom EV, Hill ML, Bouma LG, Zhang J, Crossfield IJM, Saunders N (2024) The California Legacy Survey. V. Chromospheric activity cycles in main-sequence stars. Astrophys J Suppl Ser 274(2):35. https://doi.org/10.3847/1538-4365/ad676c

Iwanek P, Soszyński I, Stępień K, Kozłowski S, Skowron J, Udalski A, Szymański MK, Wrona M, Pietrukowicz P, Poleski R, Mróz P, Ulaczyk K, Skowron DM, Gromadzki M, Rybicki K, Mróz MJ, Ratajczak M (2024) The OGLE collection of variable stars: over 18 000 rotating variables toward the Galactic bulge. Acta Astron 74(1):1–25. https://doi.org/10.32023/0001-5237/74.1.1

Jackman JAG, Shkolnik EL, Million C, Fleming S, Richey-Yowell T, Loyd ROP (2023) Extending optical flare models to the UV: results from comparing of TESS and GALEX flare observations for M dwarfs. Mon Not R Astron Soc 519(3):3564–3583. https://doi.org/10.1093/mnras/stac3135

Järvinen SP, Carroll TA, Hubrig S, Ilyin I, Schöller M (2019) New evidence for weak magnetic fields in Herbig Ae/Be stars. Mon Not R Astron Soc 489(1):886–890. https://doi.org/10.1093/mnras/stz2190

Jayasinghe T, Stanek KZ, Kochanek CS, Shappee BJ, Holoien TWS, Thompson TA, Prieto JL, Dong S, Pawlak M, Pejcha O, Shields JV, Pojmanski G, Otero S, Hurst N, Britt CA, Will D (2020) The ASAS-SN catalogue of variable stars - V. Variables in the Southern hemisphere. Mon Not R Astron Soc 491(1):13–28. https://doi.org/10.1093/mnras/stz2711

Jordan C, Kuin NPM (1988) The outer atmospheres and winds of T Tau and RU Lupi. In: Longdon N, Rolfe EJ (eds) ESA spec publ. ESA spec publ, vol 2, pp 97–100

Joy AH (1954) Variable stars of low luminosity. Publ Astron Soc Pac 66(388):5. https://doi.org/10.1086/126639

Karoff C, Metcalfe TS, Santos ÂRG, Montet BT, Isaacson H, Witzke V, Shapiro AI, Mathur S, Davies GR, Lund MN, Garcia RA, Brun AS, Salabert D, Avelino PP, van Saders J, Egeland R, Cunha MS, Campante TL, Chaplin WJ, Krivova N, Solanki SK, Stritzinger M, Knudsen MF (2018) The influence of metallicity on stellar differential rotation and magnetic activity. Astrophys J 852(1):46. https://doi.org/10.3847/1538-4357/aaa026

Kennicutt RC Jr (1998) Star formation in galaxies along the Hubble sequence. Annu Rev Astron Astrophys 36:189–232. https://doi.org/10.1146/annurev.astro.36.1.189

Klein RI, Chevalier RA (1978) X-ray bursts from type II supernovae. Astrophys J Lett 223:L109–L112. https://doi.org/10.1086/182740

Kowalski AF (2024a) Stellar flares. Living Rev Sol Phys 21(1):1. https://doi.org/10.1007/s41116-024-00039-4

Kowalski AF (2024b) Stellar flares. Living Rev Sol Phys 21(1):1. https://doi.org/10.1007/s41116-024-00039-4

Kowalski AF, Hawley SL, Wisniewski JP, Osten RA, Hilton EJ, Holtzman JA, Schmidt SJ, Davenport JRA (2013) Time-resolved properties and global trends in dMe flares from simultaneous photometry and spectra. Astrophys J Suppl Ser 207(1):15. https://doi.org/10.1088/0067-0049/207/1/15

Kowalski AF, Mathioudakis M, Hawley SL, Wisniewski JP, Dhillon VS, Marsh TR, Hilton EJ, Brown BP (2016) M dwarf flare continuum variations on one-second timescales: calibrating and modeling of ULTRACAM flare color indices. Astrophys J 820(2):95. https://doi.org/10.3847/0004-637X/820/2/95

Kowalski AF, Wisniewski JP, Hawley SL, Osten RA, Brown A, Fariña C, Valenti JA, Brown S, Xilouris M, Schmidt SJ, Johns-Krull C (2019) The near-ultraviolet continuum radiation in the impulsive phase of HF/GF-type dMe flares. I. Data. Astrophys J 871(2):167. https://doi.org/10.3847/1538-4357/aaf058

Kulkarni SR, Harrison FA, Grefenstette BW, Earnshaw HP, Andreoni I, Berg DA, Bloom JS, Cenko SB, Chornock R, Christiansen JL, Coughlin MW, Wuollet Criswell A, Darvish B, Das KK, De K, Dessart L, Dixon D, Dorsman B, El-Badry K, Evans C, Ford KES, Fremling C, Gansicke BT, Gezari S, Goetberg Y, Green GM, Graham MJ, Heida M, Ho AYQ, Jaodand AD, Johns-Krull CM, Kasliwal MM, Lazzarini M, Lu W, Margutti R, Martin DC, Masters DC, McKernan B, Naze Y, Nissanke SM, Parazin B, Perley DA, Phinney ES, Piro AL, Raaijmakers G, Rauw G, Rodriguez AC, Sana H, Senchyna P, Singer LP, Spake JJ, Stassun KG, Stern D, Teplitz HI, Weisz DR, Yao Y (2021) Science with the Ultraviolet Explorer (UVEX). arXiv e-prints. arXiv:2111.15608. https://doi.org/10.48550/arXiv.2111.15608

Lamers HJGLM, Cassinelli JP (1999) Introduction to stellar winds. Cambridge University Press

Larson RB (1995) Star formation in groups. Mon Not R Astron Soc 272(1):213–220. https://doi.org/10.1093/mnras/272.1.213

Leenaarts J, Pereira TMD, Carlsson M, Uitenbroek H, De Pontieu B (2013a) The formation of IRIS diagnostics. I. A quintessential model atom of Mg II and general formation properties of the Mg II h&k lines. Astrophys J 772(2):89. https://doi.org/10.1088/0004-637X/772/2/89

Leenaarts J, Pereira TMD, Carlsson M, Uitenbroek H, De Pontieu B (2013b) The formation of IRIS diagnostics. II. The formation of the Mg II h&k lines in the solar atmosphere. Astrophys J 772(2):90. https://doi.org/10.1088/0004-637X/772/2/90

Leitherer C, Schaerer D, Goldader JD, González Delgado RM, Robert C, Foo Kune D, de Mello DF, Devost D, Heckman TM (1999) Starburst99: synthesis models for galaxies with active star formation. Astrophys J Suppl Ser 123(1):3–40. https://doi.org/10.1086/313233

Leitherer C, Ortiz Otálvaro PA, Bresolin F, Kudritzki R-P, Lo Faro B, Pauldrach AWA, Pettini M, Rix SA (2010) A library of theoretical ultraviolet spectra of massive, hot stars for evolutionary synthesis. Astrophys J Suppl Ser 189(2):309–335. https://doi.org/10.1088/0067-0049/189/2/309

Lemmens AFP, Rutten RGM, Zwaan C (1992) Magnetic structure in cool stars. XVIII. UV-line emission from T Tauri stars. Astron Astrophys 257:671–676

Li X, Wang S, Han H, Yang H, Zheng C, Huang Y, Liu J (2024) Ultraviolet and chromospheric activity and habitability of M stars. Astrophys J 966(1):69. https://doi.org/10.3847/1538-4357/ad3038

Lignieres F, Catala C, Mangeney A (1996) Angular momentum transfer in pre-main-sequence stars of intermediate mass. Astron Astrophys 314:465–476

Linsky JL, Ayres TR (1978) Stellar model chromospheres. VI. Empirical estimates of the chromospheric radiative losses of late-type stars. Astrophys J 220:619–628. https://doi.org/10.1086/155945

Linsky JL, Bornmann PL, Carpenter KG, Wing RF, Giampapa MS, Worden SP, Hege EK (1982) Outer atmospheres of cool stars. XII. A survey of IUE ultraviolet emission line spectra of cool dwarf stars. Astrophys J 260:670–694. https://doi.org/10.1086/160288

López-Martínez F, Gómez de Castro AI (2014) Constraints to the magnetospheric properties of T Tauri stars - I. The C II], Fe II] and Si II] ultraviolet features. Mon Not R Astron Soc 442(4):2951–2962. https://doi.org/10.1093/mnras/stu1045

Loyd ROP, France K (2014) Fluctuations and flares in the ultraviolet line emission of cool stars: implications for exoplanet transit observations. Astrophys J Suppl Ser 211(1):9. https://doi.org/10.1088/0067-0049/211/1/9

Loyd ROP, France K, Youngblood A, Schneider C, Brown A, Hu R, Segura A, Linsky J, Redfield S, Tian F, Rugheimer S, Miguel Y, Froning CS (2018a) The MUSCLES treasury survey. V. FUV flares on active and inactive M dwarfs. Astrophys J 867(1):71. https://doi.org/10.3847/1538-4357/aae2bd

Loyd ROP, Shkolnik EL, Schneider AC, Barman TS, Meadows VS, Pagano I, Peacock S (2018b) HAZMAT. IV. Flares and superflares on young M stars in the far ultraviolet. Astrophys J 867(1):70. https://doi.org/10.3847/1538-4357/aae2ae

Lu YL, Curtis JL, Angus R, David TJ, Hattori S (2022) Bridging the gap—the disappearance of the intermediate period gap for fully convective stars, uncovered by new ZTF rotation periods. Astron J 164(6):251. https://doi.org/10.3847/1538-3881/ac9bee

Ludwig B, Drout MR, Götberg Y, Lang D, Laroche A (2026) The Stripped-star Ultraviolet Magellanic Cloud Survey (SUMS): the UV photometric catalog and stripped star candidate selection. Astrophys J 999:73. https://doi.org/10.3847/1538-4357/ae2d13. arXiv:2505.18632

Maeda K, Moriya T, Kawabata K, Tanaka M, Tominaga N, Nomoto K (2012) Core-collapse supernova diversities. From the weakest to most powerful explosions. Mem Soc Astron Ital 83:264

Magaudda E, Stelzer B, Covey KR, Raetz S, Matt SP, Scholz A (2020) Relation of X-ray activity and rotation in M dwarfs and predicted time-evolution of the X-ray luminosity. Astron Astrophys 638:A20. https://doi.org/10.1051/0004-6361/201937408

Martin DC, Fanson J, Schiminovich D, Morrissey P, Friedman PG, Barlow TA, Conrow T, Grange R, Jelinsky PN, Milliard B, Siegmund OHW, Bianchi L, Byun Y-I, Donas J, Forster K, Heckman TM, Lee Y-W, Madore BF, Malina RF, Neff SG, Rich RM, Small T, Surber F, Szalay AS, Welsh B, Wyder TK (2005) The Galaxy Evolution Explorer: a space ultraviolet survey mission. Astrophys J Lett 619(1):L1–L6. https://doi.org/10.1086/426387

Massana P, Ruiz-Lara T, Noël NED, Gallart C, Nidever DL, Choi Y, Sakowska JD, Besla G, Olsen KAG, Monelli M, Dorta A, Stringfellow GS, Cassisi S, Bernard EJ, Zaritsky D, Cioni MRL, Monachesi A, van der Marel RP, de Boer TJL, Walker AR (2022) The synchronized dance of the Magellanic clouds' star formation history. Mon Not R Astron Soc 513(1):L40–L45. https://doi.org/10.1093/mnrasl/slac030

Matzner CD, McKee CF (1999) The expulsion of stellar envelopes in core-collapse supernovae. Astrophys J 510(1):379–403. https://doi.org/10.1086/306571

McJunkin M, France K, Burgh EB, Herczeg GJ, Schindhelm R, Brown JM, Brown A (2013) Probing the inner regions of protoplanetary disks with CO absorption line spectroscopy. Astrophys J 766(1):12. https://doi.org/10.1088/0004-637X/766/1/12

McQuillan A, Mazeh T, Aigrain S (2014) Rotation periods of 34,030 Kepler main-sequence stars: the full autocorrelation sample. Astrophys J Suppl Ser 211(2):24. https://doi.org/10.1088/0067-0049/211/2/24

Meftah M, Damé L, Bolsée D, Hauchecorne A, Pereira N, Sluse D, Cessateur G, Irbah A, Bureau J, Weber M, Bramstedt K, Hilbig T, Thiéblemont R, Marchand M, Lefèvre F, Sarkissian A, Bekki S (2018) SOLAR-ISS: a new reference spectrum based on SOLAR/SOLSPEC observations. Astron Astrophys 611:A1. https://doi.org/10.1051/0004-6361/201731316

Miguel Y, Kaltenegger L (2014) Exploring atmospheres of hot mini-Neptunes and extrasolar giant planets orbiting different stars with application to HD 97658b, WASP-12b, CoRoT-2b, XO-1b, and HD 189733b. Astrophys J 780(2):166. https://doi.org/10.1088/0004-637X/780/2/166

Miller AE, Cioni M-RL, de Grijs R, Sun N-C, Bell CPM, Choudhury S, Ivanov VD, Marconi M, Oliveira JM, Petr-Gotzens M, Ripepi V, van Loon JT (2022) The VMC survey - XLVII. Turbulence-controlled hierarchical star formation in the Large Magellanic Cloud. Mon Not R Astron Soc 512(1):1196–1213. https://doi.org/10.1093/mnras/stac508

Milone AP, Cordoni G, Marino AF, D'Antona F, Bellini A, Di Criscienzo M, Dondoglio E, Lagioia EP, Langer N, Legnardi MV, Libralato M, Baumgardt H, Bettinelli M, Cavecchi Y, de Grijs R, Deng L, Hastings B, Li C, Mohandasan A, Renzini A, Vesperini E, Wang C, Ziliotto T, Carlos M, Costa G, Dell'Agli F, Di Stefano S, Jang S, Martorano M, Simioni M, Tailo M, Ventura P (2023) Hubble Space Telescope survey of Magellanic cloud star clusters. Photometry and astrometry of 113 clusters and early results. Astron Astrophys 672:A161. https://doi.org/10.1051/0004-6361/202244798

Mokiem MR, de Koter A, Vink JS, Puls J, Evans CJ, Smartt SJ, Crowther PA, Herrero A, Langer N, Lennon DJ, Najarro F, Villamariz MR (2007) The empirical metallicity dependence of the mass-loss rate of O- and early B-type stars. Astron Astrophys 473(2):603–614. https://doi.org/10.1051/0004-6361:20077545

Montet BT, Tovar G, Foreman-Mackey D (2017) Long-term photometric variability in Kepler full-frame images: magnetic cycles of Sun-like stars. Astrophys J 851(2):116. https://doi.org/10.3847/1538-4357/aa9e00

Moos HW, Cash WC, Cowie LL, Davidsen AF, Dupree AK, Feldman PD, Friedman SD, Green JC, Green RF, Gry C, Hutchings JB, Jenkins EB, Linsky JL, Malina RF, Michalitsianos AG, Savage BD, Shull JM, Siegmund OHW, Snow TP, Sonneborn G, Vidal-Madjar A, Willis AJ, Woodgate BE, York DG, Ake TB, Andersson B-G, Andrews JP, Barkhouser RH, Bianchi L, Blair WP, Brownsberger KR, Cha AN, Chayer P, Conard SJ, Fullerton AW, Gaines GA, Grange R, Gummin MA, Hebrard G, Kriss GA, Kruk JW, Mark D, McCarthy DK, Morbey CL, Murowinski R, Murphy EM, Oegerle WR, Ohl RG, Oliveira C, Osterman SN, Sahnow DJ, Saisse M, Sembach KR, Weaver HA, Welsh BY, Wilkinson E, Zheng W (2000) Overview of the Far Ultraviolet Spectroscopic Explorer mission. Astrophys J Lett 538(1):L1–L6. https://doi.org/10.1086/312795

Morton DC, Spitzer L Jr (1966) Line spectra of Δ and π Scorpii in the far-ultraviolet. Astrophys J 144:1. https://doi.org/10.1086/148586

Neupert WM (1965) Intensity variations in the solar extreme ultraviolet spectrum observed by OSO-1. Ann Astrophys 28:446

Neupert WM (1966) A study of active regions in the solar corona observed by OSO-I. Astron J 71:173. https://doi.org/10.1086/109889

Newton ER, Irwin J, Charbonneau D, Berlind P, Calkins ML, Mink J (2017) The Hα emission of nearby M dwarfs and its relation to stellar rotation. Astrophys J 834(1):85. https://doi.org/10.3847/1538-4357/834/1/85

Nielsen MB, Gizon L, Schunker H, Karoff C (2013) Rotation periods of 12 000 main-sequence Kepler stars: dependence on stellar spectral type and comparison with $v \sin i$ observations. Astron Astrophys 557:L10. https://doi.org/10.1051/0004-6361/201321912

Noyes RW, Hartmann LW, Baliunas SL, Duncan DK, Vaughan AH (1984) Rotation, convection, and magnetic activity in lower main-sequence stars. Astrophys J 279:763–777. https://doi.org/10.1086/161945

Oláh K, Kővári Z, Petrovay K, Soon W, Baliunas S, Kolláth Z, Vida K (2016) Magnetic cycles at different ages of stars. Astron Astrophys 590:A133. https://doi.org/10.1051/0004-6361/201628479

Olspert N, Lehtinen JJ, Käpylä MJ, Pelt J, Grigorievskiy A (2018) Estimating activity cycles with probabilistic methods. II. The Mount Wilson Ca H&K data. Astron Astrophys 619:A6. https://doi.org/10.1051/0004-6361/201732525

Osten RA, Hawley SL, Allred JC, Johns-Krull CM, Roark C (2005) From radio to X-ray: flares on the dMe flare star EV Lacertae. Astrophys J 621(1):398–416. https://doi.org/10.1086/427275

Osten RA, Kowalski A, Drake SA, Krimm H, Page K, Gazeas K, Kennea J, Oates S, Page M, de Miguel E, Novák R, Apeltauer T, Gehrels N (2016) A very bright, very hot, and very long flaring event from the M dwarf binary system DG CVn. Astrophys J 832(2):174. https://doi.org/10.3847/0004-637X/832/2/174

Pallavicini R, Golub L, Rosner R, Vaiana GS, Ayres T, Linsky JL (1981) Relations among stellar X-ray emission observed from Einstein, stellar rotation and bolometric luminosity. Astrophys J 248:279–290. https://doi.org/10.1086/159152

Parker JW, Garmany CD, Massey P, Walborn NR (1992) The stellar content of LH 9 and 10 (N11) in the LMC: a case for sequential star formation. Astron J 103:1205. https://doi.org/10.1086/116136

Parker JW, Hill JK, Cornett RH, Hollis J, Zamkoff E, Bohlin RC, O'Connell RW, Neff SG, Roberts MS, Smith AM, Stecher TP (1998) Ultraviolet Imaging Telescope observations of the Magellanic Clouds. Astron J 116(1):180–208. https://doi.org/10.1086/300419

Pellegrino C, Howell DA, Terreran G, Arcavi I, Bostroem KA, Brown PJ, Burke J, Dong Y, Gilkis A, Hiramatsu D, Hosseinzadeh G, McCully C, Modjaz M, Newsome M, Padilla Gonzalez E, Pritchard TA, Sand DJ, Valenti S, Williamson M (2022) The diverse properties of type Icn supernovae point to multiple progenitor channels. Astrophys J 938(1):73. https://doi.org/10.3847/1538-4357/ac8ff6

Pesnell WD, Thompson BJ, Chamberlin PC (2012) The Solar Dynamics Observatory (SDO). Sol Phys 275(1-2):3–15. https://doi.org/10.1007/s11207-011-9841-3

Pietrzyński G, Graczyk D, Gallenne A, Gieren W, Thompson IB, Pilecki B, Karczmarek P, Górski M, Suchomska K, Taormina M, Zgirski B, Wielgórski P, Kołaczkowski Z, Konorski P, Villanova S, Nardetto N, Kervella P, Bresolin F, Kudritzki RP, Storm J, Smolec R, Narloch W (2019) A distance to the Large Magellanic Cloud that is precise to one per cent. Nature 567(7747):200–203. https://doi.org/10.1038/s41586-019-0999-4

Pineda JS, Youngblood A, France K (2021) The far ultraviolet M-dwarf evolution survey. I. The rotational evolution of high-energy emissions. Astrophys J 911(2):111. https://doi.org/10.3847/1538-4357/abe8d7

Piro AL, Nakar E (2026) Early emission from double detonation type Ia supernovae. Astrophys J 993:63. https://doi.org/10.3847/1538-4357/ae0e6e. arXiv:2507.14290

Piro AL, Chang P, Weinberg NN (2010) Shock breakout from type Ia supernova. Astrophys J 708(1):598–604. https://doi.org/10.1088/0004-637X/708/1/598

Pizzolato N, Maggio A, Micela G, Sciortino S, Ventura P (2003) The stellar activity–rotation relationship revisited: dependence of saturated and non-saturated X-ray emission regimes on stellar mass for late-type dwarfs. Astron Astrophys 397:147–157. https://doi.org/10.1051/0004-6361:20021560

Pollin JM, Sim SA, Shingles LJ, Pakmor R, Callan FP, Collins CE, Roepke FK, Kwok LA, Holas A, Srivastav S (2026) Multidimensional nebular-phase calculations of dynamically-driven double-degenerate double-detonation models for type Ia supernovae. Mon Not R Astron Soc 548(4):stag735. https://doi.org/10.1093/mnras/stag735. arXiv:2507.05000

Praderie F, Simon T, Catala C, Boesgaard AM (1986) Short-term spectral variability in AB Aurigae: clues for activity in Herbig Ae stars. I. The ultraviolet lines of Mg II and Fe II. Astrophys J 303:311. https://doi.org/10.1086/164076

Prinja RK, Barlow MJ, Howarth ID (1990) Terminal velocities for a large sample of O stars, B supergiants, and Wolf–Rayet stars. Astrophys J 361:607. https://doi.org/10.1086/169224

Pritchard TA, Roming PWA, Brown PJ, Kuin NPM, Bayless AJ, Holland ST, Immler S, Milne P, Oates SR (2012) Early ultraviolet observations of a type IIn supernova (2007pk). Astrophys J 750(2):128. https://doi.org/10.1088/0004-637X/750/2/128

Rabinak I, Waxman E (2011) The early UV/optical emission from core-collapse supernovae. Astrophys J 728(1):63. https://doi.org/10.1088/0004-637X/728/1/63

Ranjan S, Schwieterman EW, Harman C, Fateev A, Sousa-Silva C, Seager S, Hu R (2020) Photochemistry of anoxic abiotic habitable planet atmospheres: impact of new H_2O cross sections. Astrophys J 896(2):148. https://doi.org/10.3847/1538-4357/ab9363

Raymond JC (1982) IUE observations of supernova remnants. Adv Space Res 2(9):145–151. https://doi.org/10.1016/0273-1177(82)90265-4
Reale F (2014) Coronal loops: observations and modeling of confined plasma. Living Rev Sol Phys 11(1):4. https://doi.org/10.12942/lrsp-2014-4
Reinhold T, Hekker S (2020) Stellar rotation periods from K2 campaigns 0–18. Evidence for rotation period bimodality and simultaneous variability decrease. Astron Astrophys 635:A43. https://doi.org/10.1051/0004-6361/201936887
Reinhold T, Cameron RH, Gizon L (2017) Evidence for photometric activity cycles in 3203 Kepler stars. Astron Astrophys 603:A52. https://doi.org/10.1051/0004-6361/201730599
Reinhold T, Shapiro AI, Solanki SK, Basri G (2023) New rotation period measurements of 67 163 Kepler stars. Astron Astrophys 678:A24. https://doi.org/10.1051/0004-6361/202346789
Rimmer PB, Xu J, Thompson SJ, Gillen E, Sutherland JD, Queloz D (2018) The origin of RNA precursors on exoplanets. Sci Adv 4(8):eaar3302. https://doi.org/10.1126/sciadv.aar3302
Roberge A, Lecavelier des Etangs A, Grady CA, Vidal-Madjar A, Bouret J-C, Feldman PD, Deleuil M, Andre M, Boggess A, Bruhweiler FC, Ferlet R, Woodgate B (2001) FUSE and Hubble Space Telescope/STIS observations of hot and cold gas in the AB Aurigae system. Astrophys J Lett 551(1):L97–L100. https://doi.org/10.1086/319831
Rogerson JB, Spitzer L, Drake JF, Dressler K, Jenkins EB, Morton DC, York DG (1973) Spectrophotometric results from the Copernicus satellite. I. Instrumentation and performance. Astrophys J Lett 181:L97–L102. https://doi.org/10.1086/181194
Roman-Duval J, Jackson JM, Heyer M, Rathborne J, Simon R (2010) Physical properties and Galactic distribution of molecular clouds identified in the Galactic Ring Survey. Astrophys J 723(1):492–507. https://doi.org/10.1088/0004-637X/723/1/492
Roming PWA, Kennedy TE, Mason KO, Nousek JA, Ahr L, Bingham RE, Broos PS, Carter MJ, Hancock BK, Huckle HE, Hunsberger SD, Kawakami H, Killough R, Koch TS, McLelland MK, Smith K, Smith PJ, Soto JC, Boyd PT, Breeveld AA, Holland ST, Ivanushkina M, Pryzby MS, Still MD, Stock J (2005) The Swift Ultra-Violet/Optical Telescope. Space Sci Rev 120(3-4):95–142. https://doi.org/10.1007/s11214-005-5095-4
Rotstein N, Gimenez de Castro CG (1996) Radiation-driven magnetohydrodynamic wind solutions for hot luminous stars. Astrophys J 464:859. https://doi.org/10.1086/177373
Rubele S, Pastorelli G, Girardi L, Cioni M-RL, Zaggia S, Marigo P, Bekki K, Bressan A, Clementini G, de Grijs R, Emerson J, Groenewegen MAT, Ivanov VD, Muraveva T, Nanni A, Oliveira JM, Ripepi V, Sun N-C, van Loon JT (2018) The VMC survey - XXXI: the spatially resolved star formation history of the main body of the Small Magellanic Cloud. Mon Not R Astron Soc 478(4):5017–5036. https://doi.org/10.1093/mnras/sty1279
Rugheimer S, Segura A, Kaltenegger L, Sasselov D (2015) UV surface environment of Earth-like planets orbiting FGKM stars through geological evolution. Astrophys J 806(1):137. https://doi.org/10.1088/0004-637X/806/1/137
Rutten RGM, Schrijver CJ, Lemmens AFP, Zwaan C (1991) Magnetic structure in cool stars. XVII. Minimum radiative losses from the outer atmosphere. Astron Astrophys 252:203
Saar SH, Brandenburg A (1999) Time evolution of the magnetic activity cycle period. II. Results for an expanded stellar sample. Astrophys J 524(1):295–310. https://doi.org/10.1086/307794
Sahnow DJ, Moos HW, Ake TB, Andersen J, Andersson B-G, Andre M, Artis D, Berman AF, Blair WP, Brownsberger KR, Calvani HM, Chayer P, Conard SJ, Feldman PD, Friedman SD, Fullerton AW, Gaines GA, Gawne WC, Green JC, Gummin MA, Jennings TB, Joyce JB, Kaiser ME, Kruk JW, Lindler DJ, Massa D, Murphy EM, Oegerle WR, Ohl RG, Roberts BA, Romelfanger ML, Roth KC, Sankrit R, Sembach KR, Shelton RL, Siegmund OHW, Silva CJ, Sonneborn G, Vaclavik SR, Weaver HA, Wilkinson E (2000) On-orbit performance of the Far Ultraviolet Spectroscopic Explorer satellite. Astrophys J Lett 538(1):L7–L11. https://doi.org/10.1086/312794
Sakurai T (1985) Magnetic stellar winds: a 2-D generalization of the Weber–Davis model. Astron Astrophys 152:121–129
Sakurai T (2022) Probability distribution functions of solar and stellar flares. Physics 5(1):11–23. https://doi.org/10.3390/physics5010002
Salim S, Rich RM, Charlot S, Brinchmann J, Johnson BD, Schiminovich D, Seibert M, Mallery R, Heckman TM, Forster K, Friedman PG, Martin DC, Morrissey P, Neff SG, Small T, Wyder TK, Bianchi L, Donas J, Lee Y-W, Madore BF, Milliard B, Szalay AS, Welsh BY, Yi SK (2007) UV star formation rates in the local universe. Astrophys J Suppl Ser 173(2):267–292. https://doi.org/10.1086/519218
Sander AAC (2023) The driving of hot star winds. In: Vidotto AA, Fossati L, Vink JS (eds) Winds of stars and exoplanets. IAU symposium, vol 370, pp 130–143. https://doi.org/10.1017/S1743921322004719
Sasso C, Andretta V, Spadaro D (2015) Modelling low-lying, cool solar loops with optically thick radiative losses. Astron Astrophys 583:A54. https://doi.org/10.1051/0004-6361/201526598

Schootemeijer A, Shenar T, Langer N, Grin N, Sana H, Gräfener G, Schürmann C, Wang C, Xu X-T (2024) An absence of binary companions to Wolf-Rayet stars in the Small Magellanic Cloud: implications for mass loss and black hole masses at low metallicities. Astron Astrophys 689:A157. https://doi.org/10.1051/0004-6361/202449978

Schrijver CJ (1987) Magnetic structure in cool stars. XI. Relations between radiative fluxes measuring stellar activity, and evidence for two components in stellar chromospheres. Astron Astrophys 172:111–123

Schröder K-P, Mittag M, Pérez Martínez MI, Cuntz M, Schmitt JHMM (2012) Basal chromospheric flux and Maunder Minimum-type stars: the quiet-Sun chromosphere as a universal phenomenon. Astron Astrophys 540:A130. https://doi.org/10.1051/0004-6361/201118363

Scowen PA, Jones CE, Oudmaijer RD (2022) UV spectropolarimetry for stellar, interstellar, and exoplanetary astrophysics with Polstar. Astrophys Space Sci 367(12):126. https://doi.org/10.1007/s10509-022-04143-5

Seitenzahl IR, Ciaraldi-Schoolmann F, Röpke FK, Fink M, Hillebrandt W, Kromer M, Pakmor R, Ruiter AJ, Sim SA, Taubenberger S (2013) Three-dimensional delayed-detonation models with nucleosynthesis for type Ia supernovae. Mon Not R Astron Soc 429(2):1156–1172. https://doi.org/10.1093/mnras/sts402

Senchyna P, Stark DP, Charlot S, Plat A, Chevallard J, Chen Z, Jones T, Sanders RL, Rudie GC, Cooper TJ, Bruzual G (2022) Direct constraints on the extremely metal-poor massive stars underlying nebular C IV emission from ultra-deep HST/COS ultraviolet spectroscopy. Astrophys J 930(2):105. https://doi.org/10.3847/1538-4357/ac5d38

Shkolnik EL, Barman TS (2014) HAZMAT. I. The evolution of far-UV and near-UV emission from early M stars. Astron J 148(4):64. https://doi.org/10.1088/0004-6256/148/4/64

Shulyak D, Reiners A, Engeln A, Malo L, Yadav R, Morin J, Kochukhov O (2017) Strong dipole magnetic fields in fast rotating fully convective stars. Nat Astron 1:0184. https://doi.org/10.1038/s41550-017-0184

Shvartzvald Y, Waxman E, Gal-Yam A, Ofek EO, Ben-Ami S, Berge D, Kowalski M, Bühler R, Worm S, Rhoads JE, Arcavi I, Maoz D, Polishook D, Stone N, Trakhtenbrot B, Ackermann M, Aharonson O, Birnholtz O, Chelouche D, Guetta D, Hallakoun N, Horesh A, Kushnir D, Mazeh T, Nordin J, Ofir A, Ohm S, Parsons D, Pe'er A, Perets HB, Perdelwitz V, Poznanski D, Sadeh I, Sagiv I, Shahaf S, Soumagnac M, Tal-Or L, Santen JV, Zackay B, Guttman O, Rekhi P, Townsend A, Weinstein A, Wold I (2024) ULTRASAT: a wide-field time-domain UV space telescope. Astrophys J 964(1):74. https://doi.org/10.3847/1538-4357/ad2704

Simons R, Thilker D, Bianchi L, Wyder T (2014) The ultraviolet view of the Magellanic clouds from GALEX: a first look at the LMC source catalog. Adv Space Res 53(6):939–949. https://doi.org/10.1016/j.asr.2013.07.016

Smartt SJ (2009) Progenitors of core-collapse supernovae. Annu Rev Astron Astrophys 47(1):63–106. https://doi.org/10.1146/annurev-astro-082708-101737

Stanimirovic S, Staveley-Smith L, Dickey JM, Sault RJ, Snowden SL (1999) The large-scale HI structure of the Small Magellanic Cloud. Mon Not R Astron Soc 302(3):417–436. https://doi.org/10.1046/j.1365-8711.1999.02013.x

Stanimirovic S, Staveley-Smith L, van der Hulst JM, Bontekoe TJR, Kester DJM, Jones PA (2000) Cool dust and gas in the Small Magellanic Cloud. Mon Not R Astron Soc 315(4):791–807. https://doi.org/10.1046/j.1365-8711.2000.03480.x

Stelzer B, Marino A, Micela G, López-Santiago J, Liefke C (2013) The UV and X-ray activity of the M dwarfs within 10 pc of the Sun. Mon Not R Astron Soc 431(3):2063–2079. https://doi.org/10.1093/mnras/stt225

Stelzer B, Damasso M, Scholz A, Matt SP (2016) A path towards understanding the rotation–activity relation of M dwarfs with K2 mission, X-ray and UV data. Mon Not R Astron Soc 463(2):1844–1864. https://doi.org/10.1093/mnras/stw1936

Stepien K (1994) Applicability of the Rossby number in activity–rotation relations for dwarfs and giants. Astron Astrophys 292:191–207

Subramaniam A, Choudhury S, de Grijs R, et al (2026) Star clusters in the ultraviolet. Space Sci Rev 222:58. https://doi.org/10.1007/s11214-026-01310-w

Sun N-C, de Grijs R, Subramanian S, Bekki K, Bell CPM, Cioni M-RL, Ivanov VD, Marconi M, Oliveira JM, Piatti AE, Ripepi V, Rubele S, Tatton BL, van Loon JT (2017a) The VMC survey. XXVII. Young stellar structures in the LMC's bar star-forming complex. Astrophys J 849(2):149. https://doi.org/10.3847/1538-4357/aa911e

Sun N-C, de Grijs R, Subramanian S, Cioni M-RL, Rubele S, Bekki K, Ivanov VD, Piatti AE, Ripepi V (2017b) The VMC survey. XXII. Hierarchical star formation in the 30 Doradus–N158–N159–N160 star-forming complex. Astrophys J 835(2):171. https://doi.org/10.3847/1538-4357/835/2/171

Sun N-C, de Grijs R, Cioni M-RL, Rubele S, Subramanian S, van Loon JT, Bekki K, Bell CPM, Ivanov VD, Marconi M, Muraveva T, Oliveira JM, Ripepi V (2018) The VMC survey. XXIX. Turbulence-controlled

hierarchical star formation in the Small Magellanic Cloud. Astrophys J 858(1):31. https://doi.org/10.3847/1538-4357/aabc50

Tandon SN, Hutchings JB, Ghosh SK, Subramaniam A, Koshy G, Girish V, Kamath PU, Kathiravan S, Kumar A, Lancelot JP, Mahesh PK, Mohan R, Murthy J, Nagabhushana S, Pati AK, Postma J, Rao NK, Sankarasubramanian K, Sreekumar P, Sriram S, Stalin CS, Sutaria F, Sreedhar YH, Barve IV, Mondal C, Sahu S (2017a) In-orbit performance of UVIT and first results. J Astrophys Astron 38(2):28. https://doi.org/10.1007/s12036-017-9445-x

Tandon SN, Subramaniam A, Girish V, Postma J, Sankarasubramanian K, Sriram S, Stalin CS, Mondal C, Sahu S, Joseph P, Hutchings J, Ghosh SK, Barve IV, George K, Kamath PU, Kathiravan S, Kumar A, Lancelot JP, Leahy D, Mahesh PK, Mohan R, Nagabhushana S, Pati AK, Kameswara Rao N, Sreedhar YH, Sreekumar P (2017b) In-orbit calibrations of the Ultraviolet Imaging Telescope. Astron J 154(3):128. https://doi.org/10.3847/1538-3881/aa8451

Thuillier G, Hersé M, Labs D, Foujols T, Peetermans W, Gillotay D, Simon PC, Mandel H (2003) The solar spectral irradiance from 200 to 2400 nm as measured by the SOLSPEC spectrometer from the Atlas and Eureca missions. Sol Phys 214(1):1–22. https://doi.org/10.1023/A:1024048429145

Tobias C, Santiago H (2020) Fractal dimension in star formation regions. Bolet Asoc Argentina Astron 61B:136–138. https://sedici.unlp.edu.ar/handle/10915/101509. arXiv:2008.00037

Tousey R, Bartoe JDF, Brueckner GE, Purcell JD (1977) Extreme ultraviolet spectroheliograph ATM experiment S082A. Appl Opt 16:870–878. https://doi.org/10.1364/AO.16.000870

Vardavas IM (2005) The dependence of the Rossby number and XUV–Lyα emission flux with age for solar-like G-type stars. Mon Not R Astron Soc 363(1):L51–L55. https://doi.org/10.1111/j.1745-3933.2005.00082.x

Vázquez-Semadeni E, González-Samaniego A, Colín P (2017) Hierarchical star cluster assembly in globally collapsing molecular clouds. Mon Not R Astron Soc 467(2):1313–1328. https://doi.org/10.1093/mnras/stw3229

Vernazza JE, Avrett EH, Loeser R (1981) Structure of the solar chromosphere. III. Models of the EUV brightness components of the quiet Sun. Astrophys J Suppl Ser 45:635–725. https://doi.org/10.1086/190731

Vilhu O (1984) The nature of magnetic activity in lower main sequence stars. Astron Astrophys 133:117–126

Wargelin BJ, Saar SH, Pojmański G, Drake JJ, Kashyap VL (2017) Optical, UV, and X-ray evidence for a 7-yr stellar cycle in Proxima Centauri. Mon Not R Astron Soc 464(3):3281–3296. https://doi.org/10.1093/mnras/stw2570

Waxman E, Katz B (2017) Shock breakout theory. In: Alsabti AW, Murdin P (eds) Handbook of supernovae. Springer, p 967. https://doi.org/10.1007/978-3-319-21846-5_33

Welsh BY, Wheatley JM, Seibert M, Browne SE, West AA, Siegmund OHW, Barlow TA, Forster K, Friedman PG, Martin DC, Morrissey P, Small T, Wyder T, Schiminovich D, Neff S, Rich RM (2007) The detection of M dwarf UV flare events in the GALEX data archives. Astrophys J Suppl Ser 173(2):673–681. https://doi.org/10.1086/516640

Wheatley JM, Welsh BY, Siegmund OHW, Byun Y-I, Yi S, Lee Y-W, Madore BF, Viton M, Rich RM, Bianchi L, Barlow TA, Donas J, Forster K, Friedman PG, Heckman TM, Jelinsky PN, Malina RF, Martin DC, Milliard B, Morrissey P, Neff SG, Schiminovich D, Small T, Szalay AS, Wyder TK (2005) Large-amplitude ultraviolet variations in the RR Lyrae star ROTSE-I J143753.84+345924.8. Astrophys J Lett 619(1):L123–L126. https://doi.org/10.1086/422391

Wilson OC (1968) Flux measurements at the centers of stellar H- and K-lines. Astrophys J 153:221. https://doi.org/10.1086/149652

Wilson OC (1978) Chromospheric variations in main-sequence stars. Astrophys J 226:379–396. https://doi.org/10.1086/156618

Woods TN, Tobiska WK, Rottman GJ, Worden JR (2000) Improved solar Lyman α irradiance modeling from 1947 through 1999 based on UARS observations. J Geophys Res 105(A12):27195–27216. https://doi.org/10.1029/2000JA000051

Wright NJ, Drake JJ (2016) Solar-type dynamo behaviour in fully convective stars without a tachocline. Nature 535(7613):526–528. https://doi.org/10.1038/nature18638

Wright NJ, Drake JJ, Mamajek EE, Henry GW (2011) The stellar-activity–rotation relationship and the evolution of stellar dynamos. Astrophys J 743(1):48. https://doi.org/10.1088/0004-637X/743/1/48

Wright NJ, Newton ER, Williams PKG, Drake JJ, Yadav RK (2018) The stellar rotation–activity relationship in fully convective M dwarfs. Mon Not R Astron Soc 479(2):2351–2360. https://doi.org/10.1093/mnras/sty1670

Young PR, Dere KP, Landi E, Del Zanna G, Mason HE (2016) The CHIANTI atomic database. J Phys B, At Mol Opt Phys 49(7):074009. https://doi.org/10.1088/0953-4075/49/7/074009

Youngblood A, France K, Loyd ROP, Brown A, Mason JP, Schneider PC, Tilley MA, Berta-Thompson ZK, Buccino A, Froning CS, Hawley SL, Linsky J, Mauas PJD, Redfield S, Kowalski A, Miguel Y, Newton

ER, Rugheimer S, Segura A, Roberge A, Vieytes M (2017) The MUSCLES treasury survey. IV. Scaling relations for ultraviolet, Ca II K, and energetic particle fluxes from M dwarfs. Astrophys J 843(1):31. https://doi.org/10.3847/1538-4357/aa76dd

Youngblood A, Pineda JS, France K (2021) FUMES. II. Lyα reconstructions of young, active M dwarfs. Astrophys J 911(2):112. https://doi.org/10.3847/1538-4357/abe8d8

Zapartas E, de Mink SE, Justham S, Smith N, de Koter A, Renzo M, Arcavi I, Farmer R, Götberg Y, Toonen S (2019) The diverse lives of progenitors of hydrogen-rich core-collapse supernovae: the role of binary interaction. Astron Astrophys 631:A5. https://doi.org/10.1051/0004-6361/201935854

Publisher's Note Springer Nature remains neutral with regard to jurisdictional claims in published maps and institutional affiliations.

Authors and Affiliations

Richard de Grijs[1,2,3] · Martin A. Barstow[4] · Deepak Chahal[1,2,5] · Fabio Favata[6,7,3] · Xiaoting Fu[8] · Ana I. Gómez de Castro[9] · Sipra Hota[10,11] · Firoza Sutaria[10]

✉ Richard de Grijs
richard.de-grijs@mq.edu.au

1 School of Mathematical and Physical Sciences, Macquarie University, Balaclava Road, Sydney, NSW 2109, Australia

2 Astrophysics and Space Technologies Research Centre, Macquarie University, Balaclava Road, Sydney, NSW 2109, Australia

3 International Space Science Institute–Beijing, 1 Nanertiao, Zhongguancun, Hai Dian District, Beijing 100190, China

4 School of Physics & Astronomy, University of Leicester, Leicester LE1 7RH, UK

5 Astronomy Unit, Department of Physics and Astronomy, Queen Mary University of London, Mile End Road, London E1 4NS, UK

6 INAF–Osservatorio Astronomico di Palermo, Piazza del Parlamento, 1, 90134 Palermo, Italy

7 Department of Physics, Imperial College London, Exhibition Road, London SW7 2AZ, UK

8 Purple Mountain Observatory, Chinese Academy of Sciences, Nanjing, Jiangsu 210023, China

9 Space Astronomy Research Group–AEGORA, Facultad de Ciencias Matemáticas, Universidad Complutense de Madrid, Plaza de Ciencias 3, 28040 Madrid, Spain

10 Indian Institute of Astrophysics, 2nd Block, Koramangala, Bangalore-560034, India

11 Pondicherry University, R.V. Nagar, Kalapet, Puducherry-605014, India